CHAPTER 4

VIEW FACTORS

4.1 INTRODUCTION

In many engineering applications the exchange of radiative energy between surfaces is virtually unaffected by the medium that separates them. Such (radiatively) *nonparticipating media* include vacuum as well as monatomic and most diatomic gases (including air) at low to moderate temperature levels (i.e., before ionization and dissociation occurs). Examples include spacecraft heat rejection systems, solar collector systems, radiative space heaters, illumination problems, and so on.

In the following four chapters we shall consider the analysis of *surface radiation transport,* i.e., radiative heat transfer in the absence of a participating medium, for different levels of complexity. It is common practice to simplify the analysis by making the assumption of an *idealized enclosure* and/or of *ideal surface properties*.

The greatest simplification arises if all surfaces are black: for such a situation no reflected radiation needs to be accounted for, and all emitted radiation is diffuse (i.e., the intensity leaving a surface does not depend on direction). The next level of difficulty arises if surfaces are assumed to be gray, diffuse emitters (and, thus, absorbers) as well as gray, diffuse reflectors. The vast majority of engineering calculations are limited to such ideal surfaces, which are the topic of Chapter 5.

If the reflective behavior of a surface deviates strongly from a diffuse reflector (e.g., a polished metal, which reflects almost like a mirror) one may often approximate the reflectance to consist of a purely diffuse and a purely specular component. This situation is discussed in Chapter 6. However, if greater accuracy is desired, if the reflectance cannot be approximated by purely diffuse and specular components, or if the assumption of a gray surface is not acceptable, a more general approach must be taken. A few such methods are briefly outlined in Chapter 7.

As discussed in Chapter 1 thermal radiation is generally a long-range phenomenon. This is *always* the case in the absence of a participating medium, since photons will travel unimpeded from surface to surface. Therefore, performing a thermal radiation analysis for one surface implies that all surfaces, no matter how far removed, that can exchange radiative energy with one another must be considered simultaneously. How much energy any two surfaces exchange depends in part on their size, separation distance, and orientation, leading to geometric functions known as *view factors.* In the present chapter these view factors are developed for gray, diffusely radiating (i.e., emitting and reflecting) surfaces. However, the view factor is a very basic function that will also be employed in the analysis of specular reflectors as well as for the analysis for surfaces with arbitrary emission and reflection properties.

Making an energy balance on a surface element, as shown in Fig. 4-1, we find

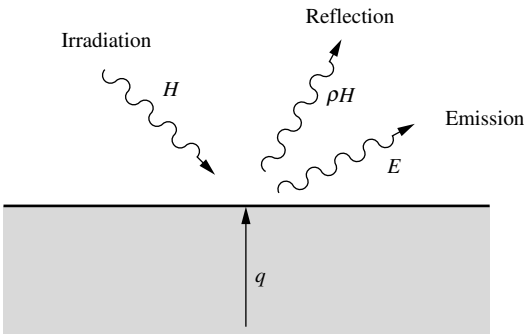

FIGURE 4-1
Surface energy balance.

$$q = q_{\text{emission}} - q_{\text{absorption}} = E - \alpha H. \tag{4.1}$$

In this relation q_{emission} and $q_{\text{absorption}}$ are absolute values with directions as given by Fig. 4-1, while q is the net heat flux supplied to the surface, as defined in Chapter 1 by equation (1.38). According to this definition q is positive if the heat is coming from inside the wall material, by conduction or other means ($q > 0$), and negative if going from the enclosure into the wall ($q < 0$). Alternatively, the heat flux may be expressed as

$$\begin{aligned} q &= q_{\text{out}} - q_{\text{in}} = (q_{\text{emission}} + q_{\text{reflection}}) - q_{\text{irradiation}} \\ &= (E + \rho H) - H, \end{aligned} \tag{4.2}$$

which is, of course, the same as equation (4.1) since, for opaque surfaces, $\rho = 1-\alpha$. The irradiation H depends, in general, on the level of emission from surfaces far removed from the point under consideration, as schematically indicated in Fig. 4-2*a*. Thus, in order to make a radiative energy balance we always need to consider an entire *enclosure* rather than an infinitesimal control volume (as is normally done for other modes of heat transfer, i.e., conduction or convection). The enclosure must be *closed* so that irradiation from all possible directions can be accounted for, and the enclosure surfaces must be *opaque* so that all irradiation is accounted for, for each direction. In practice, an incomplete enclosure may be closed by introducing artificial surfaces. An enclosure may be idealized in two ways, as indicated in Fig. 4-2*b*: by replacing a complex geometrical shape with a few simple surfaces, and by assuming surfaces to be isothermal with constant (i.e., average) heat flux values across them. Obviously, the idealized enclosure approaches the real enclosure for sufficiently small isothermal subsurfaces.

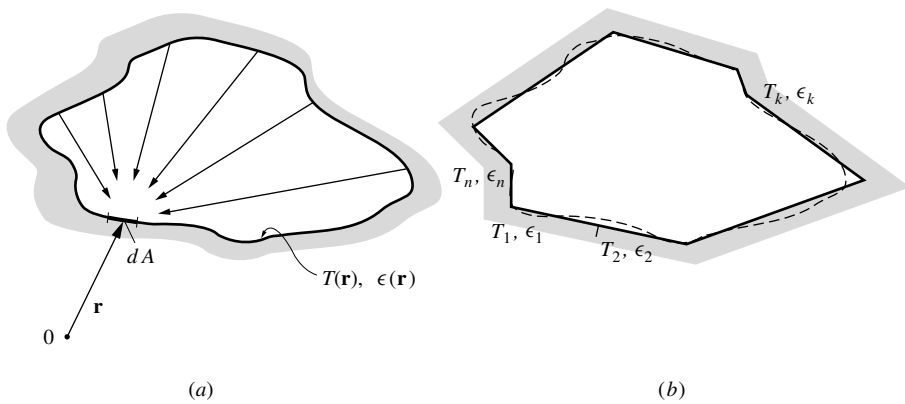

FIGURE 4-2
(a) Irradiation from different locations in an enclosure, *(b)* real and ideal enclosures for radiative transfer calculations.

4.2 DEFINITION OF VIEW FACTORS

To make an energy balance on a surface element, equation (4.1), the irradiation H must be evaluated. In a general enclosure the irradiation will have contributions from all visible parts of the enclosure surface. Therefore, we need to determine how much energy leaves an arbitrary surface element dA' that travels toward dA. The geometric relations governing this process for "diffuse" surfaces (for surfaces that absorb and emit diffusely, and also reflect radiative energy diffusely) are known as *view factors.* Other names used in the literature are *configuration factor, angle factor,* and *shape factor*, and sometimes the term *diffuse view factor* is used (to distinguish from *specular view factors* for specularly reflecting surfaces; see Chapter 6). The view factor between two infinitesimal surface elements dA_i and dA_j, as shown in Fig. 4-3, is defined as

$$dF_{dA_i-dA_j} \equiv \frac{\text{diffuse energy leaving } dA_i \text{ directly toward and intercepted by } dA_j}{\text{total diffuse energy leaving } dA_i}, \tag{4.3}$$

where the word "directly" is meant to imply "on a straight path, without intervening reflections." This view factor is infinitesimal since only an infinitesimal *fraction* can be intercepted by an infinitesimal area. From the definition of intensity and Fig. 4-3 we may determine the heat transfer rate from dA_i to dA_j as

$$I(\mathbf{r}_i)(dA_i \cos\theta_i)\, d\Omega_j = I(\mathbf{r}_i) \cos\theta_i \cos\theta_j\, dA_i\, dA_j/S^2, \tag{4.4}$$

where θ_i (or θ_j) is the angle between the surface normal $\hat{\mathbf{n}}_i$ (or $\hat{\mathbf{n}}_j$) and the line connecting dA_i and dA_j (of length S). The total radiative energy leaving dA_i into the hemisphere above it is $J = E + \rho H$, where J is called the *radiosity*. Since the surface emits and reflects diffusely both E and ρH obey equation (1.33), and the outgoing flux may be related to intensity by

$$J(\mathbf{r}_i)\, dA_i = \left[E(\mathbf{r}_i) + \rho(\mathbf{r}_i)\, H(\mathbf{r}_i)\right] dA_i = \pi I(\mathbf{r}_i)\, dA_i.$$

Note that the radiative intensity away from dA_i, due to emission and/or reflection, does not depend on direction. Therefore, the view factor between two infinitesimal areas is

$$dF_{dA_i-dA_j} = \frac{\cos\theta_i \cos\theta_j}{\pi S^2}\, dA_j. \tag{4.5}$$

By introducing the abbreviation $\mathbf{s}_{ij} = \mathbf{r}_j - \mathbf{r}_i$, and noting that $\cos\theta_i = \hat{\mathbf{n}}_i \cdot \mathbf{s}_{ij}/|\mathbf{s}_{ij}|$, the view factor may be recast in vector form as

$$dF_{dA_i-dA_j} = \frac{(\hat{\mathbf{n}}_i \cdot \mathbf{s}_{ij})(\hat{\mathbf{n}}_j \cdot \mathbf{s}_{ji})}{\pi S^4}\, dA_j. \tag{4.6}$$

Switching subscripts i and j in equation (4.5) immediately leads to the important *law of reciprocity*,

$$dA_i\, dF_{dA_i-dA_j} = dA_j\, dF_{dA_j-dA_i}. \tag{4.7}$$

Often, enclosures are idealized to consist of a number of finite isothermal subsurfaces, as indicated in Fig. 4-2*b*. Therefore, we should like to expand the definition of the view factor to include radiative exchange between one infinitesimal and one finite area, and between two finite areas. Consider first the exchange between an infinitesimal dA_i and a finite A_j, as shown in Fig. 4-4. The total energy leaving dA_i toward all of A_j is, from equation (4.4),

$$I(\mathbf{r}_i)\, dA_i \int_{A_j} \frac{\cos\theta_i \cos\theta_j}{S^2}\, dA_j,$$

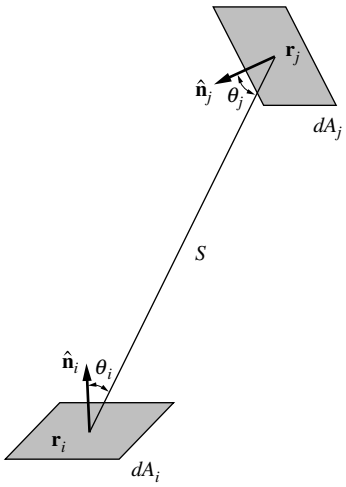

FIGURE 4-3
Radiative exchange between two infinitesimal surface elements.

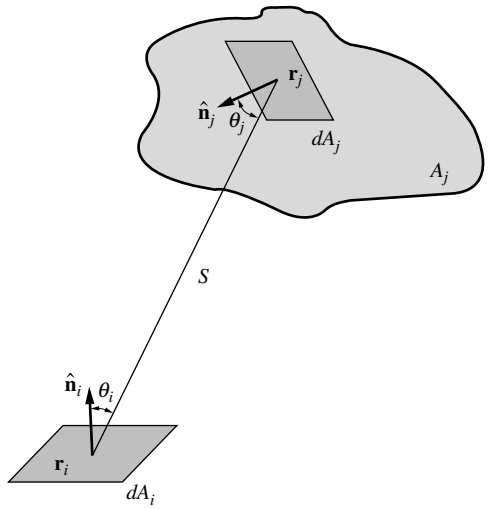

FIGURE 4-4
Radiative exchange between one infinitesimal and one finite surface element.

while the total energy leaving the dA_i into all directions remains unchanged. Thus, we find

$$F_{dA_i - A_j} = \int_{A_j} \frac{\cos\theta_i \cos\theta_j}{\pi S^2}\, dA_j, \tag{4.8}$$

which is now finite since the intercepting surface, A_j, is finite.

Next we consider the view factor from A_j to the infinitesimal dA_i. The amount of radiation leaving all of A_j toward dA_i is, from equation (4.4) (after switching subscripts i and j),

$$dA_i \int_{A_j} I(\mathbf{r}_j) \frac{\cos\theta_i \cos\theta_j}{S^2}\, dA_j,$$

and the total amount leaving A_j into all directions is

$$\pi \int_{A_j} I(\mathbf{r}_j)\, dA_j.$$

Thus, we find the view factor between surfaces A_j and dA_i is

$$dF_{A_j - dA_i} = \int_{A_j} I(\mathbf{r}_j) \frac{\cos\theta_i \cos\theta_j}{S^2}\, dA_j\, dA_i \Big/ \pi \int_{A_j} I(\mathbf{r}_j)\, dA_j, \tag{4.9}$$

which is infinitesimal since the intercepting surface, dA_i, is infinitesimal. The view factor in equation (4.9)—unlike equations (4.5) and (4.8)—is not a purely geometric parameter since it depends on the radiation field $I(\mathbf{r}_j)$. However, for an ideal enclosure as shown in Fig. 4-2*b*, it is usually assumed that the intensity leaving any surface is not only diffuse but also does not vary across the surface, i.e., $I(\mathbf{r}_j) = I_j = \text{const}$. With this assumption equation (4.9) becomes

$$dF_{A_j - dA_i} = \frac{1}{A_j} \int_{A_j} \frac{\cos\theta_i \cos\theta_j}{\pi S^2}\, dA_j\, dA_i. \tag{4.10}$$

Comparing this with equation (4.8) we find another law of reciprocity, with

$$A_j\, dF_{A_j - dA_i} = dA_i\, F_{dA_i - A_j}, \tag{4.11}$$

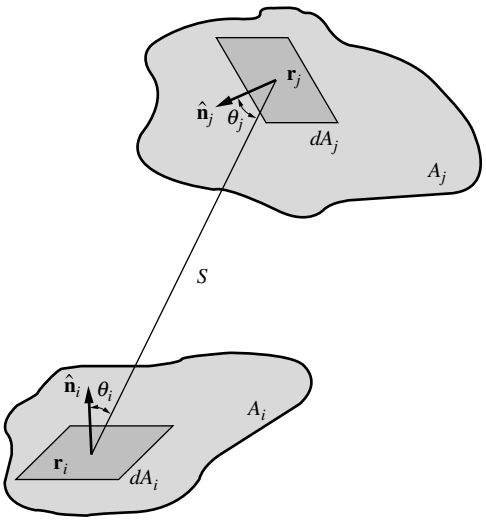

FIGURE 4-5
Radiative exchange between two finite surfaces.

subject to the restriction that the intensity leaving A_j does not vary across the surface.

Finally, we consider radiative exchange between two finite areas A_i and A_j as depicted in Fig. 4-5. The total energy leaving A_i toward A_j is, from equation (4.4),

$$\int_{A_i}\int_{A_j} I(\mathbf{r}_i)\frac{\cos\theta_i\cos\theta_j}{S^2}\,dA_j\,dA_i,$$

and the view factor follows as

$$F_{A_i-A_j} = \int_{A_i}\int_{A_j} I(\mathbf{r}_i)\frac{\cos\theta_i\cos\theta_j}{S^2}\,dA_j\,dA_i \Big/ \pi\int_{A_i} I(\mathbf{r}_i)\,dA_i. \tag{4.12}$$

If we assume again that the intensity leaving A_i does not vary across the surface, the view factor reduces to

$$F_{A_i-A_j} = \frac{1}{A_i}\int_{A_i}\int_{A_j}\frac{\cos\theta_i\cos\theta_j}{\pi S^2}\,dA_j\,dA_i. \tag{4.13}$$

The *law of reciprocity* follows readily as

$$A_i\,F_{A_i-A_j} = A_j\,F_{A_j-A_i}, \tag{4.14}$$

which is now subject to the condition that the radiation intensities leaving A_i and A_j must both be constant across their respective surfaces.

In a somewhat more compact notation, the law of reciprocity may be summarized as

$$dA_i\,dF_{di-dj} = dA_j\,dF_{dj-di}, \tag{4.15a}$$

$$dA_i\,F_{di-j} = A_j\,dF_{j-di}, \qquad (I_j = \text{const}), \tag{4.15b}$$

$$A_i\,F_{i-j} = A_j\,F_{j-i}, \qquad (I_i,\ I_j = \text{const}). \tag{4.15c}$$

The different levels of view factors may be related to one another by

$$F_{di-j} = \int_{A_j} dF_{di-dj}, \tag{4.16a}$$

$$F_{i-j} = \frac{1}{A_i}\int_{A_i} F_{di-j}\,dA_i. \tag{4.16b}$$

If the receiving surface consists of a number of subsurfaces, we also have

$$F_{i-j} = \sum_{k=1}^{K} F_{i-(j,k)}, \text{ with } A_j = \sum_{k=1}^{K} A_{(j,k)}. \tag{4.17}$$

Finally, an enclosure consisting of N surfaces, each with constant outgoing intensities, obeys the *summation relation,*

$$\sum_{j=1}^{N} F_{di-j} = \sum_{j=1}^{N} F_{i-j} = 1. \tag{4.18}$$

The last two relations follow directly from the definition of the view factor (i.e., the sum of all fractions must add up to unity). Note that equation (4.18) includes the view factor F_{i-i}. If surface A_i is flat or convex, no radiation leaving it will strike itself directly, and F_{i-i} simply vanishes. However, if A_i is concave, part of the radiation leaving it will be intercepted by itself and $F_{i-i} > 0$.

4.3 METHODS FOR THE EVALUATION OF VIEW FACTORS

The calculation of a radiative view factor between any two finite surfaces requires the solution to a double area integral, or a fourth-order integration. Such integrals are exceedingly difficult to evaluate analytically except for very simple geometries. Even numerical quadrature may often be problematic because of singularities in the integrand, and because of excessive CPU time requirements. Therefore, considerable effort has been directed toward tabulation and the development of evaluation methods for view factors. Early tables and charts for simple configurations were given by Hamilton and Morgan [1], Leuenberger and Pearson [2], and Kreith [3]. Fairly extensive tabulations were given in the books by Sparrow and Cess [4] and Siegel and Howell [5]. Siegel and Howell also give an exhaustive listing of sources for more involved view factors. The most complete tabulation is given in a catalogue by Howell [6,7], the latest version of which can also be accessed on the Internet via `http://www.engr.uky.edu/rtl/Catalog/`. A number of commercial and noncommercial computer programs for their evaluation are also available [8–18], and a review of available numerical methods has been given by Emery and coworkers [19]. Some experimental methods have been discussed by Jakob [20] and Liu and Howell [21]. Within the present book Appendix D gives view factor formulae for an extensive set of geometries. Self-contained Fortran/C++/MATLAB® programs `viewfactors` are included in Appendix F for the evaluation of all view factors listed in Appendix D [these programs call a function `view`, which may also be used from within other programs].

Radiation view factors may be determined by a variety of methods. One possible grouping of different approaches could be:

1. Direct integration:
   (*i*) analytical or numerical integration of the relations given in the previous section (surface integration);
   (*ii*) conversion of the relations to contour integrals, followed by analytical or numerical integration (contour integration).
2. Statistical determination: View factors may be determined through statistical sampling with the *Monte Carlo method*.
3. Special methods: For many simple shapes integration can be avoided by employing one of the following special methods:
   (*i*) view factor algebra, i.e., repeated application of the *rules of reciprocity* and the *summation relationship*;

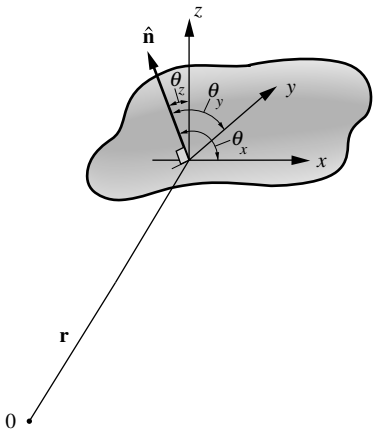

FIGURE 4-6
Unit normal and direction cosines for a surface element.

(*ii*) crossed-strings method: a simple method for evaluation of view factors in two-dimensional geometries;
(*iii*) unit sphere method: a powerful method for view factors between one infinitesimal and one finite area;
(*iv*) inside sphere method: a simple method for a few special shapes.

All of the above methods will be discussed in the following pages, except for the *Monte Carlo method,* which is treated in considerable detail in Chapter 8.

4.4 AREA INTEGRATION

To evaluate equation (4.5) or to carry out the integrations in equations (4.8) and (4.13) the integrand (i.e., $\cos\theta_i$, $\cos\theta_j$, and S) must be known in terms of a local coordinate system that describes the geometry of the two surfaces. While the evaluation of the integrand may be straightforward for some simple configurations, it is desirable to have a more generally applicable formula at one's disposal. Using an arbitrary coordinate origin, a vector pointing from the origin to a point on a surface may be written as

$$\mathbf{r} = x\hat{\mathbf{i}} + y\hat{\mathbf{j}} + z\hat{\mathbf{k}}, \tag{4.19}$$

where $\hat{\mathbf{i}}$, $\hat{\mathbf{j}}$, and $\hat{\mathbf{k}}$ are *unit vectors* pointing into the x-, y-, and z-directions, respectively. Thus the vector from dA_i going to dA_j is determined (see Fig. 4-5) as

$$\mathbf{s}_{ij} = -\mathbf{s}_{ji} = \mathbf{r}_j - \mathbf{r}_i = (x_j - x_i)\hat{\mathbf{i}} + (y_j - y_i)\hat{\mathbf{j}} + (z_j - z_i)\hat{\mathbf{k}}. \tag{4.20}$$

The length of this vector is determined as

$$|\mathbf{s}_{ij}|^2 = |\mathbf{s}_{ji}|^2 = S^2 = (x_j - x_i)^2 + (y_j - y_i)^2 + (z_j - z_i)^2. \tag{4.21}$$

We will now assume that the local surface normals are also known in terms of the unit vectors $\hat{\mathbf{i}}$, $\hat{\mathbf{j}}$, and $\hat{\mathbf{k}}$, or, from Fig. 4-6,

$$\hat{\mathbf{n}} = l\,\hat{\mathbf{i}} + m\hat{\mathbf{j}} + n\hat{\mathbf{k}}, \tag{4.22}$$

where l, m, and n are the *direction cosines* for the unit vector $\hat{\mathbf{n}}$, i.e., $l = \hat{\mathbf{n}} \cdot \hat{\mathbf{i}} = \cos\theta_x$ is the cosine of the angle θ_x between $\hat{\mathbf{n}}$ and the x-axis, etc. We may now evaluate $\cos\theta_i$ and $\cos\theta_j$ as

$$\cos\theta_i = \frac{\hat{\mathbf{n}}_i \cdot \mathbf{s}_{ij}}{S} = \frac{1}{S}\Big[(x_j - x_i)l_i + (y_j - y_i)m_i + (z_j - z_i)n_i\Big], \tag{4.23a}$$

$$\cos\theta_j = \frac{\hat{\mathbf{n}}_j \cdot \mathbf{s}_{ji}}{S} = \frac{1}{S}\Big[(x_i - x_j)l_j + (y_i - y_j)m_j + (z_i - z_j)n_j\Big]. \tag{4.23b}$$

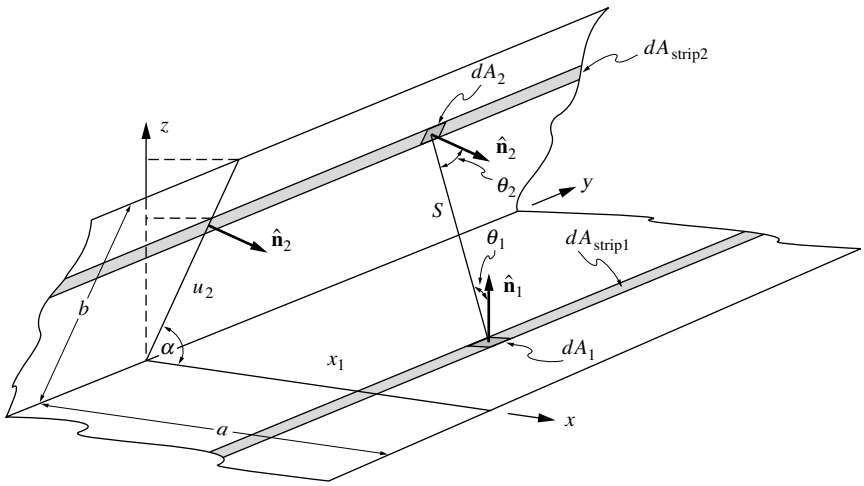

FIGURE 4-7
View factor for strips on an infinitely long groove.

Example 4.1. Consider the infinitely long ($-\infty < y < +\infty$) wedge-shaped groove as shown in Fig. 4-7. The groove has sides of widths a and b and an opening angle α. Determine the view factor between the narrow strips shown in the figure.

Solution
After placing the coordinate system as shown in the figure, we find $z_1 = 0$, $x_2 = u_2 \cos\alpha$, and $z_2 = u_2 \sin\alpha$, leading to

$$\begin{aligned} S^2 &= (x_1 - u_2\cos\alpha)^2 + (y_1 - y_2)^2 + u_2^2 \sin^2\alpha \\ &= (x_1^2 - 2x_1u_2\cos\alpha + u_2^2) + (y_1 - y_2)^2 = S_0^2 + (y_1 - y_2)^2, \end{aligned}$$

where S_0 is the projection of S in the x-z-plane and is constant in the present problem. The two surface normals are readily determined as

$$\begin{aligned} \hat{\mathbf{n}}_1 &= \hat{\mathbf{k}}, \quad \text{or} \quad l_1 = m_1 = 0, \quad n_1 = 1, \\ \hat{\mathbf{n}}_2 &= \hat{\mathbf{i}}\sin\alpha - \hat{\mathbf{k}}\cos\alpha, \quad \text{or} \quad l_2 = \sin\alpha,\ m_2 = 0,\ n_2 = -\cos\alpha, \end{aligned}$$

leading to

$$\begin{aligned} \cos\theta_1 &= u_2 \sin\alpha / S, \\ \cos\theta_2 &= [(x_1 - u_2\cos\alpha)\sin\alpha + u_2 \sin\alpha\ \cos\alpha]\,/S\ = x_1 \sin\alpha / S. \end{aligned}$$

For illustrative purposes we will first calculate $dF_{d1-\text{strip}\,2}$ from equation (4.8), and then $dF_{\text{strip}\,1-\text{strip}\,2}$ from equation (4.16). Thus

$$dF_{d1-\text{strip}\,2} = \int_{dA_{\text{strip}\,2}} \frac{\cos\theta_1 \cos\theta_2}{\pi S^2}\, dA_2 = \frac{du_2}{\pi} \int_{-\infty}^{+\infty} \frac{x_1 u_2 \sin^2\alpha\, dy_2}{\left[S_0^2 + (y_1 - y_2)^2\right]^2}$$

$$= \frac{x_1 u_2\ \sin^2\alpha\, du_2}{\pi} \left[\frac{y_2 - y_1}{2S_0^2\left[S_0^2 + (y_1 - y_2)^2\right]} + \frac{1}{2S_0^3} \tan^{-1} \frac{y_2 - y_1}{S_0} \right]_{-\infty}^{+\infty}$$

$$= \frac{x_1 u_2\ \sin^2\alpha\, du_2}{2S_0^3} = \frac{1}{2} \frac{u_2 \sin\alpha}{S_0} \frac{x_1 \sin\alpha}{S_0} \frac{du_2}{S_0} = \frac{1}{2} \cos\theta_{10} \cos\theta_{20} \frac{du_2}{S_0},$$

where θ_{10} and θ_{20} are the projections of θ_1 and θ_2 in the x-z-plane. Looking at Fig. 4-8 this may be rewritten as

$$dF_{d1-\text{strip}\,2} = \tfrac{1}{2} \cos\phi\, d\phi,$$

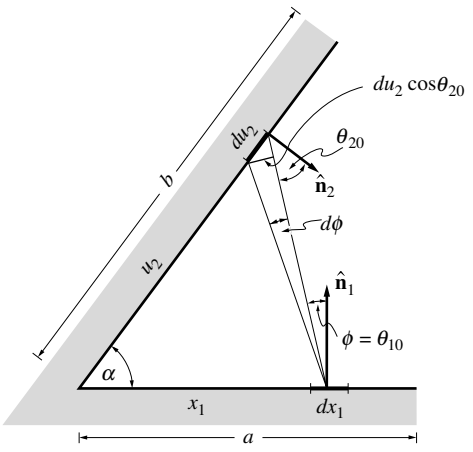

FIGURE 4-8
Two-dimensional wedge-shaped groove with projected distances.

where $\phi = \theta_{10}$ is the off-normal angle at which $dA_{\text{strip}\,2}$ is oriented from $dA_{\text{strip}\,1}$. We note that $dF_{d1-\text{strip}\,2}$ does not depend on y_1. No matter where on *strip 1* an observer is standing, he sees the same *strip 2* extending from $-\infty$ to $+\infty$. It remains to calculate $dF_{\text{strip}\,1-\text{strip}\,2}$ from equation (4.16). Since equation (4.16) simply takes an average, and since $dF_{d1-\text{strip}\,2}$ does not vary along $dA_{\text{strip}\,1}$, it follows immediately that

$$dF_{\text{strip}\,1-\text{strip}\,2} = \tfrac{1}{2}\cos\phi\, d\phi = \frac{x_1 \sin^2\alpha\, u_2\, du_2}{2S_0^3}.$$

Example 4.2. Determine the view factor F_{1-2} for the infinitely long groove shown in Fig. 4-8.

Solution
Since we already know the view factor between two infinite strips, we can write

$$F_{\text{strip}\,1-2} = \int_0^b dF_{\text{strip}\,1-\text{strip}\,2},$$
$$F_{1-2} = \frac{1}{a}\int_0^a F_{\text{strip}\,1-2}\, dx_1.$$

Therefore, from Example 4.1,

$$F_{\text{strip}\,1-2} = \frac{x_1\sin^2\alpha}{2}\int_0^b \frac{u_2\, du_2}{(x_1^2 - 2x_1u_2\cos\alpha + u_2^2)^{3/2}} = \frac{x_1\sin^2\alpha}{2}\left.\frac{x_1\cos\alpha\, u_2 - x_1^2}{x_1^2\sin^2\alpha\sqrt{x_1^2 - 2x_1u_2\cos\alpha + u_2^2}}\right|_0^b$$
$$= \frac{1}{2}\left(1 + \frac{b\cos\alpha - x_1}{\sqrt{x_1^2 - 2bx_1\cos\alpha + b^2}}\right).$$

Finally, carrying out the second integration we obtain

$$F_{1-2} = \frac{1}{a}\int_0^a F_{\text{strip}\,1-2}\, dx_1 = \frac{1}{2}\left(1 - \frac{1}{a}\sqrt{x_1^2 - 2bx_1\cos\alpha + b^2}\Big|_0^a\right) = \frac{1}{2}\left(1 + \frac{b}{a} - \sqrt{1 - 2\frac{b}{a}\cos\alpha + \left(\frac{b}{a}\right)^2}\right).$$

Example 4.3. As a final example for area integration we shall consider the view factor between two parallel, coaxial disks of radius R_1 and R_2, respectively, as shown in Fig. 4-9.

Solution
Placing x-, y-, and z-axes as shown in the figure, and making a coordinate transformation to cylindrical

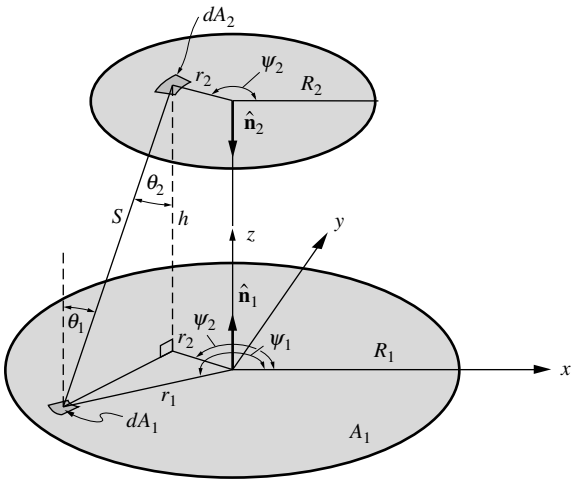

FIGURE 4-9
Coordinate systems for the view factor between parallel, coaxial disks.

coordinates, we find

$$\begin{aligned} x_1 &= r_1\cos\psi_1,\ y_1 = r_1\sin\psi_1,\ z_1 = 0; \quad dA_1 = r_1\,dr_1\,d\psi_1; \\ x_2 &= r_2\cos\psi_2,\ y_2 = r_2\sin\psi_2,\ z_2 = h; \quad dA_2 = r_2\,dr_2\,d\psi_2; \\ S^2 &= (r_1\cos\psi_1 - r_2\cos\psi_2)^2 + (r_1\sin\psi_1 - r_2\sin\psi_2)^2 + h^2 \\ &= h^2 + r_1^2 + r_2^2 - 2r_1r_2\cos(\psi_1 - \psi_2). \end{aligned}$$

Since $\hat{\mathbf{n}}_1 = \hat{\mathbf{k}}$ and $\hat{\mathbf{n}}_2 = -\hat{\mathbf{k}}$, we also find $l_1 = l_2 = m_1 = m_2 = 0$, $n_1 = -n_2 = 1$, and from equation (4.23) $\cos\theta_1 = \cos\theta_2 = h/S$. Thus, from equation (4.13)

$$F_{1-2} = \frac{1}{(\pi R_1^2)\pi}\int_{r_1=0}^{R_1}\int_{r_2=0}^{R_2}\int_{\psi_1=0}^{2\pi}\int_{\psi_2=0}^{2\pi}\frac{h^2 r_1 r_2\,d\psi_2\,d\psi_1\,dr_2\,dr_1}{\left[h^2+r_1^2+r_2^2-2r_1r_2\cos(\psi_1-\psi_2)\right]^2}.$$

Changing the dummy variable ψ_2 to $\psi = \psi_1 - \psi_2$ makes the integrand independent of ψ_1(integrating from $\psi_1 - 2\pi$ to ψ_1 is the same as integrating from 0 to 2π, since integration is over a full period), so that the ψ_1-integration may be carried out immediately:

$$F_{1-2} = \frac{2h^2}{\pi R_1^2}\int_{r_1=0}^{R_1}\int_{r_2=0}^{R_2}\int_{\psi=0}^{2\pi}\frac{r_1 r_2\,d\psi\,dr_2\,dr_1}{(h^2+r_1^2+r_2^2-2r_1r_2\cos\psi)^2}.$$

This result can also be obtained by physical argument, since the view factor from any pie slice of A_1 must be the same (and equal to the one from the entire disk). While a second integration (over r_1, r_2, or ψ) can be carried out, analytical evaluation of the remaining two integrals appears bleak. We shall abandon the problem here in the hope of finding another method with which we can evaluate F_{1-2} more easily.

4.5 CONTOUR INTEGRATION

According to *Stokes' theorem*, as developed in standard mathematics texts such as Wylie [22], a surface integral may be converted to an equivalent contour integral (see Fig. 4-10) through

$$\oint_\Gamma \mathbf{f}\cdot d\mathbf{s} = \int_A (\nabla\times\mathbf{f})\cdot\hat{\mathbf{n}}\,dA, \tag{4.24}$$

where $\mathbf{f}$ is a vector function defined everywhere on the surface A, including its boundary Γ, $\hat{\mathbf{n}}$ is the unit surface normal, and $\mathbf{s}$ is the position vector for a point on the boundary of A ($d\mathbf{s}$, therefore, is the vector describing the boundary contour of A). By convention the contour integration in

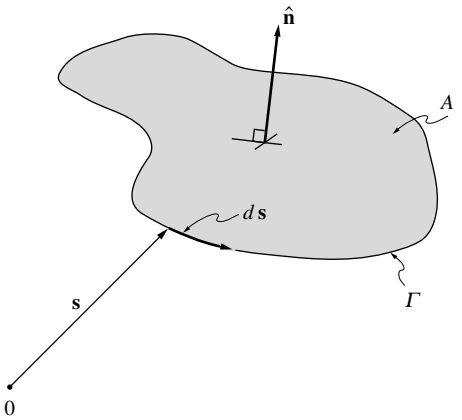

FIGURE 4-10
Conversion between surface and contour integral; Stokes' theorem.

equation (4.24) is carried out in the counterclockwise sense for an observer standing atop the surface (i.e., on the side from which the normal points up).

If a vector function **f** that makes the integrand of equation (4.24) equivalent to the one of equation (4.8) can be identified, then the area (or double) integral of equation (4.8) can be reduced to a contour (or single) integral. Applying Stokes' theorem twice, the double area integration of equation (4.13) could be converted to a double line integral. Contour integration was first applied to radiative view factor calculations (in the field of illumination engineering) by Moon [23]. The earliest applications to radiative heat transfer appear to have been by de Bastos [24] and Sparrow [25].

View Factors from Differential Elements to Finite Areas

For this case the vector function **f** may be identified as

$$\mathbf{f} = \frac{1}{2\pi}\frac{\mathbf{s}_{12}\times\hat{\mathbf{n}}_1}{S^2}, \tag{4.25}$$

leading to

$$F_{d1-2} = \frac{1}{2\pi}\oint_{\Gamma_2}\frac{(\mathbf{s}_{12}\times\hat{\mathbf{n}}_1)\cdot d\mathbf{s}_2}{S^2}, \tag{4.26}$$

where $\mathbf{s}_{12}$ is the vector pointing from dA_1 to a point on the contour of A_2 (described by vector $\mathbf{s}_2$), while $d\mathbf{s}_2$ points along the contour of A_2.

For the interested reader with some background in vector calculus we shall briefly prove that equation (4.26) is equivalent to equation (4.8). Using the identity (given, e.g., by Wylie [22]),

$$\nabla\times(\varphi\mathbf{a}) = \varphi\nabla\times\mathbf{a} - \mathbf{a}\times\nabla\varphi, \tag{4.27}$$

we may write[1]

$$2\pi\nabla_2\times\mathbf{f} = \nabla_2\times\left(\frac{\mathbf{s}_{12}\times\hat{\mathbf{n}}_1}{S^2}\right) = \frac{1}{S^2}\nabla_2\times(\mathbf{s}_{12}\times\hat{\mathbf{n}}_1) - (\mathbf{s}_{12}\times\hat{\mathbf{n}}_1)\times\nabla_2\left(\frac{1}{S^2}\right). \tag{4.28}$$

From equations (4.20) and (4.21) it follows that

$$\nabla_2\left(\frac{1}{S^2}\right) = -\frac{2}{S^3}\nabla_2 S = -\frac{2}{S^3}\frac{\mathbf{s}_{12}}{S} = -\frac{2\mathbf{s}_{12}}{S^4}.$$

[1]We add the subscript 2 to all operators to make clear that differentiation is with respect to position coordinates on A_2, for example, x_2, y_2, and z_2 if a Cartesian coordinate system is employed.

We also find, using standard vector identities,

$$(\mathbf{s}_{12} \times \hat{\mathbf{n}}_1) \times \mathbf{s}_{12} = \hat{\mathbf{n}}_1(\mathbf{s}_{12} \cdot \mathbf{s}_{12}) - \mathbf{s}_{12}(\mathbf{s}_{12} \cdot \hat{\mathbf{n}}_1) = S^2\hat{\mathbf{n}}_1 - \mathbf{s}_{12}(\mathbf{s}_{12} \cdot \hat{\mathbf{n}}_1), \tag{4.29a}$$

$$\boldsymbol{\nabla}_2 \times (\mathbf{s}_{12} \times \hat{\mathbf{n}}_1) = \hat{\mathbf{n}}_1 \cdot \boldsymbol{\nabla}_2\mathbf{s}_{12} - \mathbf{s}_{12} \cdot \boldsymbol{\nabla}_2\hat{\mathbf{n}}_1 + \mathbf{s}_{12}\boldsymbol{\nabla}_2 \cdot \hat{\mathbf{n}}_1 - \hat{\mathbf{n}}_1\boldsymbol{\nabla}_2 \cdot \mathbf{s}_{12}. \tag{4.29b}$$

In the last expression the terms $\boldsymbol{\nabla}_2\hat{\mathbf{n}}_1$ and $\boldsymbol{\nabla}_2 \cdot \hat{\mathbf{n}}_1$ drop out since $\hat{\mathbf{n}}_1$ is independent of surface A_2. Also, from equation (4.20) we find

$$\boldsymbol{\nabla}_2 \cdot \mathbf{s}_{12} = 3, \quad \boldsymbol{\nabla}_2\mathbf{s}_{12} = \hat{\mathbf{i}}\hat{\mathbf{i}} + \hat{\mathbf{j}}\hat{\mathbf{j}} + \hat{\mathbf{k}}\hat{\mathbf{k}} = \boldsymbol{\delta}, \tag{4.30}$$

where $\boldsymbol{\delta}$ is the unit tensor whose diagonal elements are unity and whose nondiagonal elements are zero:

$$\boldsymbol{\delta} = \begin{pmatrix} 1 & 0 & 0 \\ 0 & 1 & 0 \\ 0 & 0 & 1 \end{pmatrix}. \tag{4.31}$$

With $\hat{\mathbf{n}}_1 \cdot \boldsymbol{\delta} = \hat{\mathbf{n}}_1$ equation (4.29*b*) reduces to

$$\boldsymbol{\nabla}_2 \times (\mathbf{s}_{12} \times \hat{\mathbf{n}}_1) = \hat{\mathbf{n}}_1 - 3\hat{\mathbf{n}}_1 = -2\hat{\mathbf{n}}_1.$$

Substituting all this into equation (4.28), we obtain

$$2\pi\boldsymbol{\nabla}_2 \times \mathbf{f} = -\frac{2\hat{\mathbf{n}}_1}{S^2} + \frac{2}{S^4}\left[S^2\hat{\mathbf{n}}_1 - \mathbf{s}_{12}(\mathbf{s}_{12} \cdot \hat{\mathbf{n}}_1)\right] = -\frac{2}{S^4}\mathbf{s}_{12}(\mathbf{s}_{12} \cdot \hat{\mathbf{n}}_1),$$

and

$$(\boldsymbol{\nabla}_2 \times \mathbf{f}) \cdot \hat{\mathbf{n}}_2 = -\frac{(\mathbf{s}_{12} \cdot \hat{\mathbf{n}}_1)(\mathbf{s}_{12} \cdot \hat{\mathbf{n}}_2)}{\pi S^4} = \frac{\cos\theta_1 \cos\theta_2}{\pi S^2}. \tag{4.32}$$

Together with Stokes' theorem this completes the proof that equation (4.26) is equivalent to an area integral over the function given by equation (4.32).

For a Cartesian coordinate system, using equations (4.19) through (4.22), we have

$$d\mathbf{s}_2 = dx_2\hat{\mathbf{i}} + dy_2\hat{\mathbf{j}} + dz_2\hat{\mathbf{k}},$$

and equation (4.26) becomes

$$F_{d1-2} = \frac{l_1}{2\pi}\oint_{\Gamma_2}\frac{(z_2-z_1)\,dy_2 - (y_2-y_1)\,dz_2}{S^2} + \frac{m_1}{2\pi}\oint_{\Gamma_2}\frac{(x_2-x_1)\,dz_2 - (z_2-z_1)\,dx_2}{S^2} + \frac{n_1}{2\pi}\oint_{\Gamma_2}\frac{(y_2-y_1)\,dx_2 - (x_2-x_1)\,dy_2}{S^2}. \tag{4.33}$$

Example 4.4. Determine the view factor F_{d1-2} for the configuration shown in Fig. 4-11.

Solution

With the coordinate system as shown in the figure we have

$$S = \sqrt{x^2 + y^2 + c^2},$$

and, with $\hat{\mathbf{n}}_1 = -\hat{\mathbf{k}}$, or $l_1 = m_1 = 0$ and $n_1 = -1$, it follows that equation (4.33) reduces to

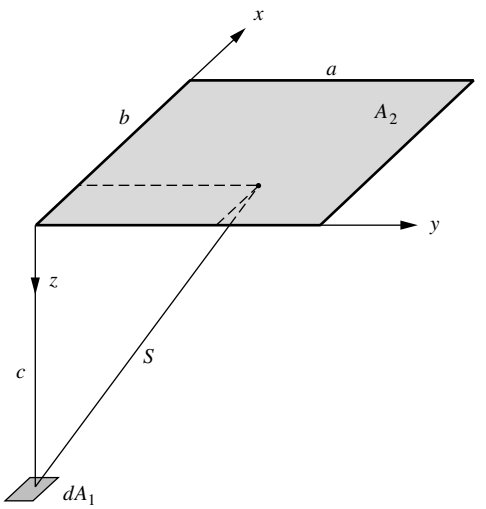

FIGURE 4-11
View factor to a rectangular plate from a parallel infinitesimal area element located opposite a corner.

$$
\begin{aligned}
F_{d1-2} &= -\frac{1}{2\pi}\oint_{\Gamma_2}\frac{y\,dx - x\,dy}{S^2} \\
&= -\frac{1}{2\pi}\left\{\left[\int_{x=0}^{x=b}\frac{y}{S^2}\,dx\right]_{y=0} + \left[\int_{y=0}^{y=a}\frac{(-x)}{S^2}\,dy\right]_{x=b} + \left[\int_{x=b}^{x=0}\frac{y}{S^2}\,dx\right]_{y=a} + \left[\int_{y=a}^{y=0}\frac{(-x)}{S^2}\,dy\right]_{x=0}\right\} \\
&= \frac{1}{2\pi}\left(\int_{y=0}^{a}\frac{b\,dy}{b^2+y^2+c^2} + \int_{x=0}^{b}\frac{a\,dx}{x^2+a^2+c^2}\right) \\
&= \frac{1}{2\pi}\left(\frac{b}{\sqrt{b^2+c^2}}\tan^{-1}\frac{y}{\sqrt{b^2+c^2}}\bigg|_0^a + \frac{a}{\sqrt{a^2+c^2}}\tan^{-1}\frac{x}{\sqrt{a^2+c^2}}\bigg|_0^b\right) \\
F_{d1-2} &= \frac{1}{2\pi}\left(\frac{b}{\sqrt{b^2+c^2}}\tan^{-1}\frac{a}{\sqrt{b^2+c^2}} + \frac{a}{\sqrt{b^2+c^2}}\tan^{-1}\frac{b}{\sqrt{a^2+c^2}}\right).
\end{aligned}
$$

View Factors between Finite Areas

To reduce the order of integration for the determination of the view factor between two finite surfaces A_1 and A_2, Stokes' theorem may be applied twice, leading to

$$A_1F_{1-2} = \frac{1}{2\pi}\oint_{\Gamma_1}\oint_{\Gamma_2}\ln S\,d\mathbf{s}_2\cdot d\mathbf{s}_1, \tag{4.34}$$

where the contours of the two surfaces are described by the two vectors $\mathbf{s}_1$ and $\mathbf{s}_2$. To prove that equation (4.34) is equivalent to equation (4.13) we get, comparing with equation (4.24) (for surface A_1),

$$\mathbf{f} = \frac{1}{2\pi}\oint_{\Gamma_2}\ln S\,d\mathbf{s}_2. \tag{4.35}$$

Taking the curl leads, by means of equation (4.27), to

$$
\begin{aligned}
2\pi\nabla_1\times\mathbf{f} &= \oint_{\Gamma_2}\nabla_1\times(\ln S\,d\mathbf{s}_2) = \oint_{\Gamma_2}\nabla_1(\ln S)\times d\mathbf{s}_2 \\
&= \oint_{\Gamma_2}\frac{1}{S}\nabla_1 S\times d\mathbf{s}_2,
\end{aligned}
\tag{4.36}
$$

where differentiation is with respect to the coordinates of surface A_1 (for which Stokes' theorem has been applied). Forming the dot product with $\hat{\mathbf{n}}_1$ then results in

$$\hat{\mathbf{n}}_1 \cdot (\boldsymbol{\nabla}_1 \times \mathbf{f}) = \oint_{\Gamma_2} \frac{1}{2\pi S} \hat{\mathbf{n}}_1 \cdot (\boldsymbol{\nabla}_1 S \times d\mathbf{s}_2) = \oint_{\Gamma_2} \frac{\hat{\mathbf{n}}_1 \times \boldsymbol{\nabla}_1 S}{2\pi S} \cdot d\mathbf{s}_2, \tag{4.37}$$

where use has been made of the vector relationship

$$\mathbf{u} \cdot (\mathbf{v} \times \mathbf{w}) = (\mathbf{u} \times \mathbf{v}) \cdot \mathbf{w}. \tag{4.38}$$

Again, from equations (4.20) and (4.21) it follows that $\boldsymbol{\nabla}_1 S = -\mathbf{s}_{12}/S$, so that

$$\begin{aligned} \hat{\mathbf{n}}_1 \cdot (\boldsymbol{\nabla}_1 \times \mathbf{f}) &= -\oint_{\Gamma_2} \frac{\hat{\mathbf{n}}_1 \times \mathbf{s}_{12}}{2\pi S^2} \cdot d\mathbf{s}_2 = \oint_{\Gamma_2} \frac{\mathbf{s}_{12} \times \hat{\mathbf{n}}_1}{2\pi S^2} \cdot d\mathbf{s}_2 \\ &= F_{d1-2} = \int_{A_2} \frac{\cos\theta_1 \cos\theta_2}{\pi S^2}\, dA_2, \end{aligned}$$

where equation (4.26) has been employed. Finally,

$$A_1 F_{1-2} = \int_{A_1} \hat{\mathbf{n}}_1 \cdot (\boldsymbol{\nabla}_1 \times \mathbf{f})\, dA_1 = \int_{A_1}\int_{A_2} \frac{\cos\theta_1 \cos\theta_2}{\pi S^2}\, dA_2\, dA_1, \tag{4.39}$$

which is, of course, identical to equation (4.13).

For Cartesian coordinates, with $\mathbf{s}_1$ and $\mathbf{s}_2$ from equation (4.19), equation (4.34) becomes

$$A_1 F_{1-2} = \frac{1}{2\pi} \oint_{\Gamma_1} \oint_{\Gamma_2} \ln S\, (dx_2\, dx_1 + dy_2\, dy_1 + dz_2\, dz_1). \tag{4.40}$$

Example 4.5. Determine the view factor between two parallel, coaxial disks, Example 4.3, by contour integration.

Solution

With $d\mathbf{s} = dx\,\hat{\mathbf{i}} + dy\,\hat{\mathbf{j}} + dz\,\hat{\mathbf{k}}$ it follows immediately from the coordinates given in Example 4.3 that

$$\begin{aligned} d\mathbf{s}_1 &= R_1\, d\psi_1(-\sin\psi_1 \hat{\mathbf{i}} + \cos\psi_1 \hat{\mathbf{j}}), \\ d\mathbf{s}_2 &= R_2\, d\psi_2(-\sin\psi_2 \hat{\mathbf{i}} + \cos\psi_2 \hat{\mathbf{j}}), \\ d\mathbf{s}_1 \cdot d\mathbf{s}_2 &= R_1 R_2\, d\psi_1\, d\psi_2(\sin\psi_1 \sin\psi_2 + \cos\psi_1 \cos\psi_2) \\ &= R_1 R_2 \cos(\psi_1 - \psi_2)\, d\psi_1\, d\psi_2, \end{aligned}$$

where, it should be remembered, $d\mathbf{s}$ is along the periphery of a disk, i.e., at $r = R$. Substituting the last expression into equation (4.34) leads to

$$F_{1-2} = \frac{R_1 R_2}{2\pi(\pi R_1^2)} \int_{\psi_1=0}^{2\pi} \int_{\psi_2=0}^{-2\pi} \ln\left[h^2 + R_1^2 + R_2^2 - 2R_1 R_2 \cos(\psi_1 - \psi_2)\right]^{1/2} \cos(\psi_1 - \psi_2)\, d\psi_2\, d\psi_1,$$

where the integration for ψ_2 is from 0 to -2π since, for an observer standing on top of A_2, the integration must be in a counterclockwise sense. Just like in Example 4.3, we can eliminate one of the integrations immediately since the angles appear only as differences, i.e., $\psi_1 - \psi_2$:

$$F_{1-2} = -\frac{1}{\pi}\frac{R_2}{R_1} \int_0^{2\pi} \ln\left(h^2 + R_1^2 + R_2^2 - 2R_1 R_2 \cos\psi\right)^{1/2} \cos\psi\, d\psi.$$

Integrating by parts we obtain:

$$\begin{aligned} F_{1-2} &= -\frac{1}{\pi}\frac{R_2}{R_1} \left[\sin\psi \ln\left(h^2 + R_1^2 + R_2^2 - 2R_1 R_2 \cos\psi\right)^{1/2} \Big|_0^{2\pi} - R_1 R_2 \int_0^{2\pi} \frac{\sin^2\psi\, d\psi}{h^2 + R_1^2 + R_2^2 - 2R_1 R_2 \cos\psi} \right] \\ &= \frac{R_2/R_1}{2\pi} \int_0^{2\pi} \frac{\sin^2\psi\, d\psi}{X - \cos\psi}, \end{aligned}$$

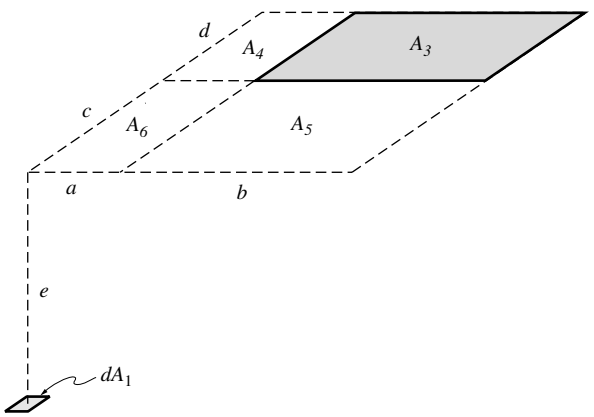

FIGURE 4-12
View factor configuration for Example 4.6.

where we have introduced the abbreviation

$$X = \frac{h^2 + R_1^2 + R_2^2}{2R_1R_2}.$$

The integral can be found in better integral tables, or may be converted to a simpler form through trigonometric relations, leading to

$$F_{1-2} = \frac{R_2/R_1}{2\pi} 2\pi \left(X - \sqrt{X^2 - 1}\right) = \frac{R_2}{R_1}\left(X - \sqrt{X^2 - 1}\right).$$

4.6 VIEW FACTOR ALGEBRA

Many view factors for fairly complex configurations may be calculated without any integration by simply using the rules of reciprocity and summation, and perhaps the known view factor for a more basic geometry. That is, besides one (or more) known view factor we will only use the following three basic equations:

Reciprocity Rule: $$A_i F_{i-j} = A_j F_{j-i}, \tag{4.15c}$$

Summation Relation: $$\sum_{j=1}^{N} F_{i-j} = 1, \tag{4.18}$$

Subsurface Summation $A_j = \sum_{k=1}^{K} A_{(j,k)}$: $$F_{i-j} = \sum_{k=1}^{K} F_{i-(j,k)} \tag{4.17}$$

We shall illustrate the usefulness of this *view factor algebra* through a few simple examples.

Example 4.6. Suppose we have been given the view factor for the configuration shown in Fig. 4-11, that is, $F_{d1-2} = F(a, b, c)$ as determined in Example 4.4. Determine the view factor F_{d1-3} for the configuration shown in Fig. 4-12.

Solution
To express F_{d1-3} in terms of known view factors $F(a, b, c)$ (with the differential area opposite one of the corners of the large plate), we fill the plane of A_3 with hypothetical surfaces A_4, A_5, and A_6 as indicated in Fig. 4-12. From the definition of view factors, or equation (4.13), it follows that

$$F_{d1-(3+4+5+6)} = F_{d1-3} + F_{d1-4} + F_{d1-(5+6)},$$
$$F_{d1-4} = F_{d1-(4+6)} - F_{d1-6}.$$

Thus,

$$F_{d1-3} = F_{d1-(3+4+5+6)} - F_{d1-(4+6)} + F_{d1-6} - F_{d1-(5+6)}.$$

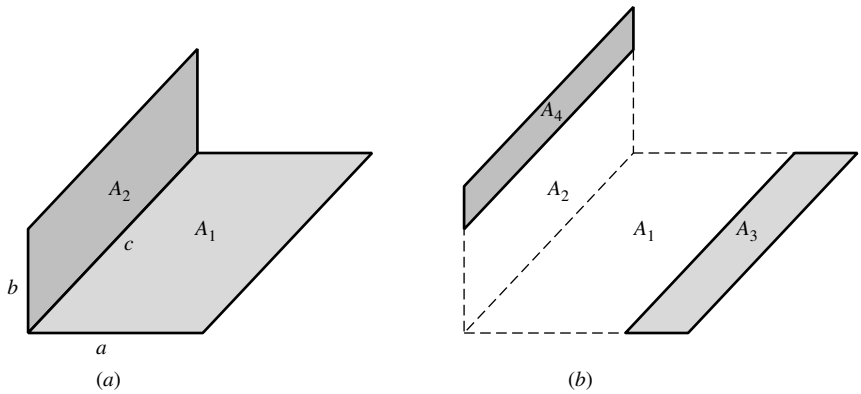

FIGURE 4-13
Configuration for Example 4.7: (*a*) full corner piece, (*b*) strips on a corner piece.

All four of these are of the type discussed in Example 4.4. Therefore,

$$F_{d1-3} = F(a+b,\, c+d,\, e) - F(a,\, c+d,\, e) + F(a,\, c,\, e) - F(a+b,\, c,\, e).$$

We have successfully converted the present complex view factor to a summation of four known, more basic ones.

Example 4.7. Assuming the view factor for a finite corner, as shown in Fig. 4-13*a*, is known as $F_{1-2} = f(a, b, c)$, where f is a known function of the dimensions of the corner pieces (as given in Appendix D), determine the view factor F_{3-4}, between the two perpendicular strips as shown in Fig. 4-13*b*.

Solution
From the definition of the view factor, and since the energy traveling to A_4 is the energy going to A_2 plus A_4 minus the energy going to A_2, it follows that

$$F_{3-4} = F_{3-(2+4)} - F_{3-2},$$

and, using reciprocity,

$$F_{3-4} = \frac{1}{A_3}\left[(A_2 + A_4)F_{(2+4)-3} - A_2F_{2-3}\right].$$

Similarly, we find

$$F_{3-4} = \frac{A_2 + A_4}{A_3}\left(F_{(2+4)-(1+3)} - F_{(2+4)-1}\right) - \frac{A_2}{A_3}\left(F_{2-(1+3)} - F_{2-1}\right).$$

All view factors on the right-hand side are corner pieces and are, thus, known by evaluating the function f with appropriate dimensions.

Example 4.8. Again, assuming the view factor is known for the configuration in Fig. 4-13*a*, determine F_{1-6} as shown in Fig. 4-14.

Solution
Examining Fig. 4-14, and employing reciprocity, we find

$$\begin{aligned}(A_5 + A_6)F_{(5+6)-(1+2)} &= (A_5 + A_6)\left(F_{(5+6)-1} + F_{(5+6)-2}\right)\\ &= A_1(F_{1-5} + F_{1-6}) + A_2(F_{2-5} + F_{2-6})\\ &= A_1\left(F_{1-(3+5)} - F_{1-3}\right) + A_2\left(F_{2-(4+6)} - F_{2-4}\right) + A_1F_{1-6} + A_2F_{2-5}.\end{aligned}$$

On the other hand, we also have

$$(A_5 + A_6)\,F_{(5+6)-(1+2)} = (A_1 + A_2)\left(F_{(1+2)-(3+4+5+6)} - F_{(1+2)-(3+4)}\right).$$

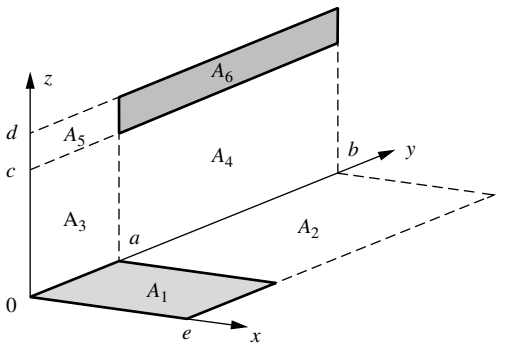

FIGURE 4-14
Configuration for Example 4.8.

In both expressions all view factors, with the exceptions of F_{1-6} and F_{2-5}, are of the type given in Fig. 4-13*a*.

These last two view factors may be related to one another, as is easily seen from their integral forms. From equation (4.13) we have

$$A_2F_{2-5} = \int_{A_2}\int_{A_5} \frac{\cos\theta_2 \cos\theta_5}{\pi S^2}\, dA_5\, dA_2.$$

With a coordinate system as shown in Fig. 4-14, we get from equations (4.21) and (4.23) $S^2 = x_2^2 + (y_2 - y_5)^2 + z_5^2$, $\cos\theta_2 = z_5/S$, $\cos\theta_5 = x_2/S$, or

$$A_2F_{2-5} = \int_{x_2=0}^{e}\int_{y_2=a}^{b}\int_{y_5=0}^{a}\int_{z_5=c}^{d} \frac{x_2 z_5\, dz_5\, dy_5\, dy_2\, dx_2}{\pi\left[x_2^2+(y_2-y_5)^2+z_5^2\right]^2}.$$

Similarly, we obtain for F_{1-6}

$$A_1F_{1-6} = \int_{x_1=0}^{e}\int_{y_1=0}^{a}\int_{y_6=a}^{b}\int_{z_6=c}^{d} \frac{x_1 z_6\, dz_6\, dy_6\, dy_1\, dx_1}{\pi\left[x_1^2+(y_1-y_6)^2+z_6^2\right]^2}.$$

Switching the names for dummy integration variables, it is obvious that

$$A_2F_{2-5} = A_1F_{1-6},$$

which may be called the *law of reciprocity for diagonally opposed pairs* of perpendicular rectangular plates.

Finally, solving for F_{1-6} we obtain

$$F_{1-6} = \frac{A_1 + A_2}{2A_1}\left(F_{(1+2)-(3+4+5+6)} - F_{(1+2)-(3+4)}\right) - \frac{1}{2}\left(F_{1-(3+5)} - F_{1-3}\right) - \frac{A_2}{2A_1}\left(F_{2-(4+6)} - F_{2-4}\right).$$

Using similar arguments, one may also determine the view factor between two arbitrarily orientated rectangular plates lying in perpendicular planes (Fig. 4-15*a*) or in parallel planes (Fig. 4-15*b*). After considerable algebra, one finds [1]:

Perpendicular plates (Fig. 4-15*a*):

$$\begin{aligned} 2A_1F_{1-2} =& f(x_2, y_2, z_3) - f(x_2, y_1, z_3) - f(x_1, y_2, z_3) + f(x_1, y_1, z_3) \\ &+ f(x_1, y_2, z_2) - f(x_1, y_1, z_2) - f(x_2, y_2, z_2) + f(x_2, y_1, z_2) \\ &- f(x_2, y_2, z_3 - z_1) + f(x_2, y_1, z_3 - z_1) + f(x_1, y_2, z_3 - z_1) - f(x_1, y_1, z_3 - z_1) \\ &+ f(x_2, y_2, z_2 - z_1) - f(x_2, y_1, z_2 - z_1) - f(x_1, y_2, z_2 - z_1) + f(x_1, y_1, z_2 - z_1), \end{aligned} \tag{4.41}$$

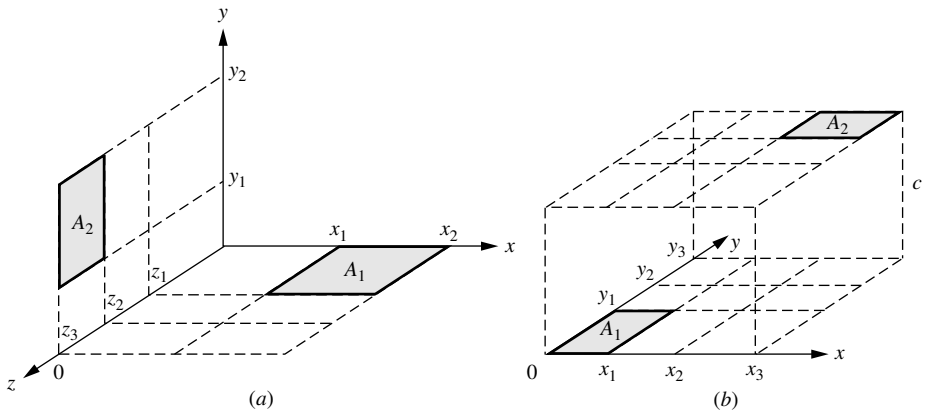

FIGURE 4-15
View factors between generalized rectangles: (*a*) surfaces are on perpendicular planes, (*b*) surfaces are on parallel planes.

where $f(w,h,l) = A_1F_{1-2}$ is the product of area and view factor between two perpendicular rectangles with a common edge as given by Configuration 39 in Appendix D.

Parallel plates (Fig. 4-15*b*):

$$\begin{aligned} 4A_1F_{1-2} =& f(x_3,y_3) - f(x_3,y_2) - f(x_3,y_3-y_1) + f(x_3,y_2-y_1) \\ & - [f(x_2,y_3) - f(x_2,y_2) - f(x_2,y_3-y_1) + f(x_2,y_2-y_1)] \\ & - [f(x_3-x_1,y_3) - f(x_3-x_1,y_2) - f(x_3-x_1,y_3-y_1) + f(x_3-x_1,y_2-y_1)] \\ & + f(x_2-x_1,y_3) - f(x_2-x_1,y_2) - f(x_2-x_1,y_3-y_1) + f(x_2-x_1,y_2-y_1), \end{aligned} \tag{4.42}$$

where $f(a,b) = A_1F_{1-2}$ is the product of area and view factor between two directly opposed, parallel rectangles, as given by Configuration 38 in Appendix D.

Equations (4.41) and (4.42) are not restricted to $x_3 > x_2 > x_1$, and so on, but hold for arbitrary values, for example, they are valid for partially overlapping surfaces. Fortran functions `perpplates` and `parlplates` are included in Appendix F for the evaluation of these view factors, based on calls to Fortran function `view` (i.e., calls to function `view` to evaluate the various view factors for Configurations 39 and 38, respectively).

Example 4.9. Show that equation (4.42) reduces to the correct expression for directly opposing rectangles.

Solution
For directly opposing rectangles, we have $x_1 = x_3 = a$, $y_1 = y_3 = b$, and $x_2 = y_2 = 0$. We note that the formula for A_1F_{1-2} for Configuration 38 in Appendix D is such that $f(a,b) = f(-a,b) = f(a,-b) = f(-a,-b)$, i.e., the view factor and area are both "negative" for a single negative dimension, making their product positive, and similarly if both a and b are negative. Also, if either a or b is zero (zero area), then $f(a,b) = 0$. Thus,

$$\begin{aligned} 4A_1F_{1-2} =& f(a,b) - 0 - 0 + f(a,-b) - [0 - 0 - 0 + 0] \\ & - [0 - 0 - 0 + 0] + f(-a,b) - 0 - 0 + f(-a,-b) \\ =& 4f(a,b). \end{aligned}$$

Many other view factors for a multitude of configurations may be obtained through view factor algebra. A few more examples will be given in this and the following chapters (when radiative exchange between black, gray-diffuse, and gray-specular surfaces is discussed).

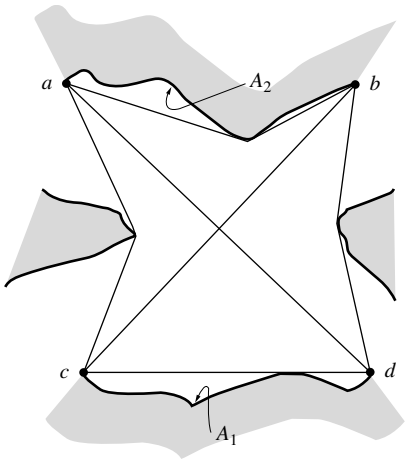

FIGURE 4-16
The crossed-strings method for arbitrary two-dimensional configurations.

4.7 THE CROSSED-STRINGS METHOD

View factor algebra may be used to determine all view factors in long enclosures with constant cross-section. The method is credited to Hottel [26],* and is called the crossed-strings method since the view factors can be determined experimentally by a person armed with four pins, a roll of string, and a yardstick. Consider the configuration in Fig. 4-16, which shows the cross-section of an infinitely long enclosure, continuing into and out of the plane of the figure: We would like to determine F_{1-2}. Obviously, the surfaces shown are rather irregular (partly convex, partly concave), and the view between them may be obstructed. We shudder at the thought of having to carry out the view factor determination by integration, and plant our four pins at the two ends of each surface, as indicated by the labels a, b, c, and d. We now connect points a and c and b and d with tight strings, making sure that no visual obstruction remains between the two strings. Similarly, we place tight strings ab and cd across the surfaces, and ad and bc diagonally between them, as shown in Fig. 4-16. Now assuming the strings to be imaginary surfaces A_{ab}, A_{ac}, and A_{bc}, we apply the summation rule to the "triangle" abc:

$$A_{ab}F_{ab-ac} + A_{ab}F_{ab-bc} = A_{ab}, \tag{4.43a}$$

$$A_{ac}F_{ac-ab} + A_{ac}F_{ac-bc} = A_{ac}, \tag{4.43b}$$

$$A_{bc}F_{bc-ac} + A_{bc}F_{bc-ab} = A_{bc}, \tag{4.43c}$$

where $F_{ab-ab} = F_{ac-ac} = F_{bc-bc} = 0$ since a tightened string will *always* form a convex surface. Equations (4.43) are three equations in six unknown view factors, which may be solved by applying reciprocity to three of them:

$$A_{ab}F_{ab-ac} + A_{ab}F_{ab-bc} = A_{ab}, \tag{4.44a}$$

$$A_{ab}F_{ab-ac} + A_{ac}F_{ac-bc} = A_{ac}, \tag{4.44b}$$

$$A_{ac}F_{ac-bc} + A_{ab}F_{ab-bc} = A_{bc}. \tag{4.44c}$$

---

* **Hoyte Clark Hottel (1903–1998)**
American engineer. Obtained his M.S. from the Massachusetts Institute of Technology in 1924, and was on the Chemical Engineering faculty at M.I.T. from 1927 until his death. While Hottel is credited with the method's discovery, he has stated that he found it in a publication while in the M.I.T. library; but, by the time he first published it, he was unable to rediscover its source. Hottel's major contributions have been his pioneering work on radiative heat transfer in furnaces, particularly his study of the radiative properties of molecular gases (Chapter 11) and his development of the zonal method (Chapter 18).

Adding the first two equations and subtracting the last leads to the *view factor for an arbitrarily shaped triangle with convex surfaces*,

$$F_{ab-ac} = \frac{A_{ab} + A_{ac} - A_{bc}}{2A_{ab}}, \tag{4.45}$$

which states that the view factor between two surfaces in an arbitrary "triangle" is equal to the area of the originating surface, plus the area of the receiving surface, minus the area of the third surface, divided by twice the originating surface.

Applying equation (4.45) to triangle *abd* we find immediately

$$F_{ab-bd} = \frac{A_{ab} + A_{bd} - A_{ad}}{2A_{ab}}. \tag{4.46}$$

But, from the summation rule,

$$F_{ab-ac} + F_{ab-bd} + F_{ab-cd} = 1. \tag{4.47}$$

Thus

$$\begin{aligned} F_{ab-cd} &= 1 - \frac{A_{ab} + A_{ac} - A_{bc}}{2A_{ab}} - \frac{A_{ab} + A_{bd} - A_{ad}}{2A_{ab}} \\ &= \frac{(A_{bc} + A_{ad}) - (A_{ac} + A_{bd})}{2A_{ab}}. \end{aligned} \tag{4.48}$$

Inspection of Fig. 4-16 shows that all radiation leaving A_{ab} traveling to A_{cd} will hit surface A_1. At the same time all radiation from A_{ab} going to A_1 must pass through A_{cd}. Therefore,

$$F_{ab-cd} = F_{ab-1}.$$

Using reciprocity and repeating the argument for surfaces A_{ab} and A_2, we find

$$F_{ab-cd} = F_{ab-1} = \frac{A_1}{A_{ab}} F_{1-ab} = \frac{A_1}{A_{ab}} F_{1-2},$$

and, finally,

$$F_{1-2} = \frac{(A_{bc} + A_{ad}) - (A_{ac} + A_{bd})}{2A_1}. \tag{4.49}$$

This formula is easily memorized by looking at the configuration between any two surfaces as a generalized "rectangle," consisting of A_1, A_2, and the two sides A_{ac} and A_{bd}. Then

$$F_{1-2} = \frac{\text{diagonals} - \text{sides}}{2 \times \text{originating area}}. \tag{4.50}$$

Example 4.10. Calculate F_{1-2} for the configuration shown in Fig. 4-17.

Solution

From the figure it is obvious that

$$s_1^2 = (c - d\cos\alpha)^2 + d^2 \sin^2\alpha = c^2 + d^2 - 2cd\cos\alpha.$$

Similarly, we have

$$\begin{aligned} s_2^2 &= (a + c)^2 + (b + d)^2 - 2(a + c)(b + d)\cos\alpha, \\ d_1^2 &= (a + c)^2 + d^2 - 2(a + c)d\cos\alpha, \\ d_2^2 &= c^2 + (b + d)^2 - 2c(b + d)\cos\alpha, \end{aligned}$$

and

$$F_{1-2} = \frac{d_1 + d_2 - (s_1 + s_2)}{2a}.$$

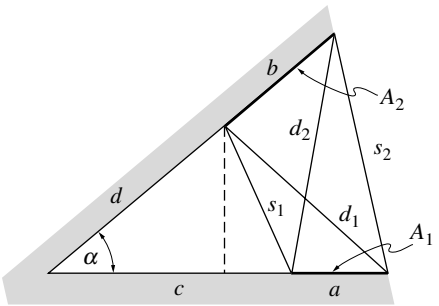

FIGURE 4-17
Infinitely long wedge-shaped groove for Examples 4.10 and 4.11.

For $c = d = 0$, this reduces to the result of Example 4.2, or

$$F_{1-2} = \frac{a + b - \sqrt{a^2 + b^2 - 2ab\cos\alpha}}{2a}.$$

Example 4.11. Find the view factor F_{d1-2} of Fig. 4-17 for the case that A_1 is an infinitesimal strip of width dx. Use the crossed-strings method.

Solution
We can obtain the result right away by replacing a by dx in the previous example. Throwing out differentials of second and higher order, we find that s_1 and d_2 remain unchanged, and

$$\begin{aligned} d_1 &= \sqrt{(c+dx)^2 + d^2 - 2(c+dx)\,d\cos\alpha} \\ &\simeq \sqrt{c^2 + d^2 - 2cd\cos\alpha + 2(c - d\cos\alpha)\,dx} \\ &\simeq \sqrt{c^2+d^2-2cd\cos\alpha}\left[1 + \frac{(c - d\cos\alpha)\,dx}{c^2 + d^2 - 2cd\cos\alpha}\right] = s_1 + \frac{dx}{s_1}(c - d\cos\alpha) \end{aligned}$$

$$\begin{aligned} s_2 &= \sqrt{(c+dx)^2 + (b+d)^2 - 2(c+dx)(b+d)\cos\alpha} \\ &\simeq d_2 + \frac{dx}{d_2}\left[c - (b+d)\cos\alpha\right]. \end{aligned}$$

Substituting this into equation (4.50), we obtain

$$\begin{aligned} F_{d1-2} &= \frac{s_1 + (c - d\cos\alpha)\,dx/s_1 + d_2 - s_1 - d_2 - [c-(b+d)\cos\alpha]\,dx/d_2}{2\,dx} \\ &= \frac{1}{2}\left[\frac{c - d\cos\alpha}{\sqrt{c^2 + d^2 - 2cd\cos\alpha}} - \frac{c - (b+d)\cos\alpha}{\sqrt{c^2 + (b+d)^2 - 2c(b+d)\cos\alpha}}\right]. \end{aligned}$$

The same result could also have been obtained by letting

$$F_{d1-2} = \lim_{a\to 0} F_{1-2},$$

where F_{1-2} is the view factor from the previous example. Using de l'Hopital's rule to determine the value of the resulting expression leads to

$$F_{d1-2} = \frac{1}{2}\left(\frac{\partial d_1}{\partial a} - \frac{\partial s_2}{\partial a}\right)\bigg|_{a=0},$$

and the above result.

Thus, the crossed-strings method may also be applied to strips. Example 4.1 could also have been solved this way; since the result is infinitesimal this computation would require retaining differentials up to second order. However, integration becomes simpler for strips of differential widths, while application of the crossed-strings method becomes more involved.

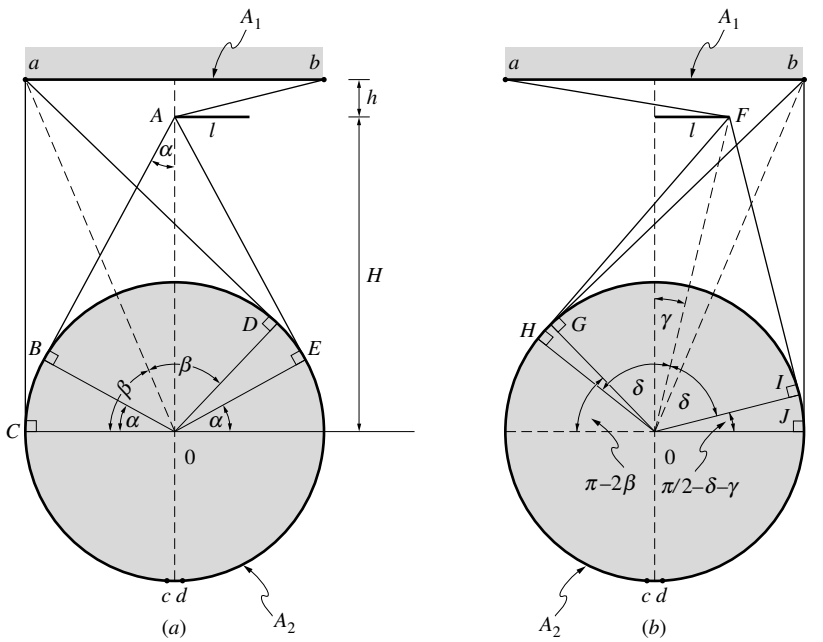

FIGURE 4-18
Configuration for view factor calculation of Example 4.12; string placement (*a*) for F^l_{1-2}, (*b*) for F^r_{1-2}.

We shall present one final example to show how view factors for curved surfaces and for configurations with floating obstructions can be determined by the crossed-strings method.

Example 4.12. Determine the view factor F_{1-2} for the configuration shown in Fig. 4-18.

Solution
In the figure the end points of A_1 and A_2 (pin points) have been labeled a, b, c, and d, and other strategic points have been labeled with capital letters. A closed-contour surface such as a cylinder may be modeled by placing two pins right next to each other, with surface A_2 being a strongly bulging convex surface between the pins. While the location of the two pins on the cylinder is arbitrary, it is usually more convenient to pick a location out of sight of A_1. Since A_1 can see A_2 from both sides of the obstruction, F_{1-2} cannot be determined with a single set of strings. Using view factor algebra, we can state that

$$F_{1-2} = F^l_{1-2} + F^r_{1-2},$$

where F^l_{1-2} and F^r_{1-2} are the view factors between A_1 and A_2 when considering only light paths on the left or right of the obstruction, respectively. The placement of strings for F^l_{1-2} is given in Fig. 4-18*a*, and for F^r_{1-2} in Fig. 4-18*b*.

Considering first F^l_{1-2}, the diagonals and sides may be determined from

$$d_1 = aD + DE + Ed, \quad d_2 = bA + AB + BC + Cc,$$

$$s_1 = aC + Cc, \qquad s_2 = bA + AE + Ed.$$

Substituting these expressions into equation (4.50) and canceling those terms that appear in a diagonal as well as in a side (Ed, bA, and Cc), we obtain

$$F^l_{1-2} = \frac{aD + DE + AB + BC - (aC + AE)}{2ab}.$$

Looking at Fig. 4-18*a* we also notice that $aC = aD$ and $AB = AE$, so that

$$F^l_{1-2} = \frac{BC + DE}{2ab} = \frac{\alpha R + (\pi - 2\beta - \alpha)R}{2 \times 2R} = \frac{1}{2}\left(\frac{\pi}{2} - \beta\right).$$

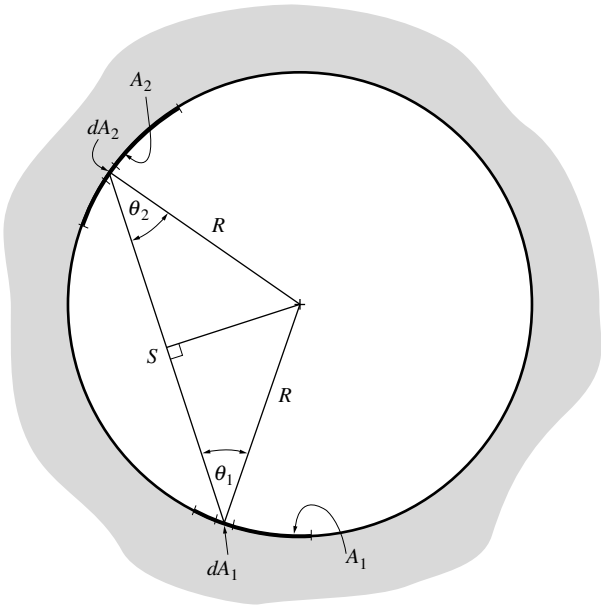

FIGURE 4-19
The inside sphere method.

But $\cot\beta = \tan(\pi/2 - \beta) = R/(h + H)$. Thus,

$$F^l_{1-2} = \frac{1}{2}\tan^{-1}\frac{R}{h+H}.$$

Similarly, we find from Fig. 4-18*b* for F^r_{1-2},

$$d_1 = aF + FI + IJ + Jd, \quad d_2 = bG + GH + Hc,$$

$$s_1 = aF + FH + Hc, \qquad s_2 = bJ + Jd,$$

$$F^r_{1-2} = \frac{FI + IJ + bG + GH - (FH + bJ)}{2ab}.$$

By inspection $bG = bJ$ and $FI = FH$, leading to

$$F^r_{1-2} = \frac{IJ + GH}{2ab} = \frac{\left(\frac{\pi}{2} - \delta - \gamma\right)R + \left(\pi - 2\beta + \delta - \frac{\pi}{2} - \gamma\right)R}{2 \times 2R}$$

$$= \frac{1}{2}\left(\frac{\pi}{2} - \beta - \gamma\right) = \frac{1}{2}\left(\tan^{-1}\frac{R}{h+H} - \tan^{-1}\frac{l}{h}\right).$$

Note that this formula only holds as long as $GH > 0$ (i.e., as long as the cylinder is seen without obstruction from point b). Finally, adding the left and right contributions to the view factor,

$$F_{1-2} = \tan^{-1}\frac{R}{h+H} - \frac{1}{2}\tan^{-1}\frac{l}{h}.$$

4.8 THE INSIDE SPHERE METHOD

Consider two surfaces A_1 and A_2 that are both parts of the surface of one and the same sphere, as shown in Fig. 4-19. We note that, for this type of configuration, $\theta_1 = \theta_2 = \theta$ and $S = 2R\cos\theta$. Therefore,

$$F_{d1-2} = \int_{A_2} \frac{\cos\theta_1 \cos\theta_2}{\pi S^2}\, dA_2 = \int_{A_2} \frac{\cos^2\theta}{\pi(2R\cos\theta)^2}\, dA_2 = \frac{1}{4\pi R^2}\int_{A_2} dA_2 = \frac{A_2}{A_s}, \tag{4.51}$$

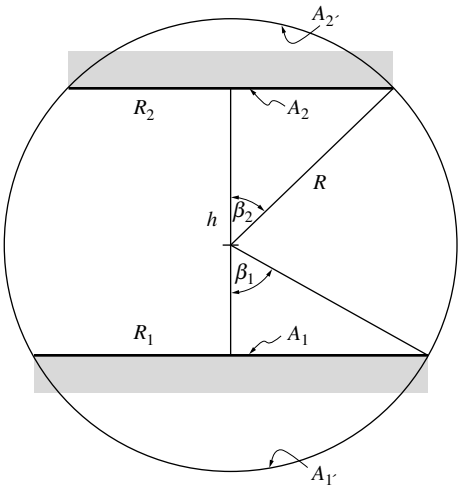

FIGURE 4-20
View factor between coaxial parallel disks.

where $A_s = 4\pi R^2$ is the surface area of the entire sphere. Similarly, from equation (4.16),

$$F_{1-2} = F_{d1-2} = \frac{A_2}{A_s}, \tag{4.52}$$

since F_{d1-2} does not depend on the position of dA_1. Therefore, because of the unique geometry of a sphere, the view factor between two surfaces on the same sphere only depends on the *size* of the receiving surface, and not on the *location* of either one.

The inside sphere method is primarily used in conjunction with view factor algebra, to determine the view factor between two surfaces that may not necessarily lie on a sphere.

Example 4.13. Find the view factor between two parallel, coaxial disks of radius R_1 and R_2 using the inside sphere method.

Solution

Inspecting Fig. 4-20 we see that it is possible to place the parallel disks inside a sphere of radius R in such a way that the entire peripheries of both disks lie on the surface of the sphere.

Since all radiation from A_1 to A_2 travels on to the spherical cap $A_{2'}$ (in the absence of A_2), and since all radiation from A_1 to $A_{2'}$ must pass through A_2, we have

$$F_{1-2} = F_{1-2'}.$$

Using reciprocity and applying a similar argument for A_1 and spherical cap $A_{1'}$, we find

$$F_{1-2} = F_{1-2'} = \frac{A_{2'}}{A_1} F_{2'-1} = \frac{A_{2'}}{A_1} F_{2'-1'} = \frac{A_{1'} A_{2'}}{A_1 A_s}.$$

The areas of the spherical caps are readily calculated as

$$A_{i'} = 2\pi R^2 \int_0^{\beta_i} \sin\beta \, d\beta = 2\pi R^2 (1 - \cos\beta_i), \quad i = 1, 2.$$

Thus, with $A_1 = \pi R_1^2$ and $A_s = 4\pi R^2$, this results in

$$F_{1-2} = \frac{(2\pi R^2)^2 (1 - \cos\beta_1)(1 - \cos\beta_2)}{\pi R_1^2 \, 4\pi R^2}.$$

From Fig. 4-20 one finds (assuming $\beta_i \le \pi/2$) $\cos\beta_i = \sqrt{R^2 - R_i^2}/R$, and

$$F_{1-2} = \frac{1}{R_1^2} \left(R - \sqrt{R^2 - R_1^2} \right) \left(R - \sqrt{R^2 - R_2^2} \right).$$

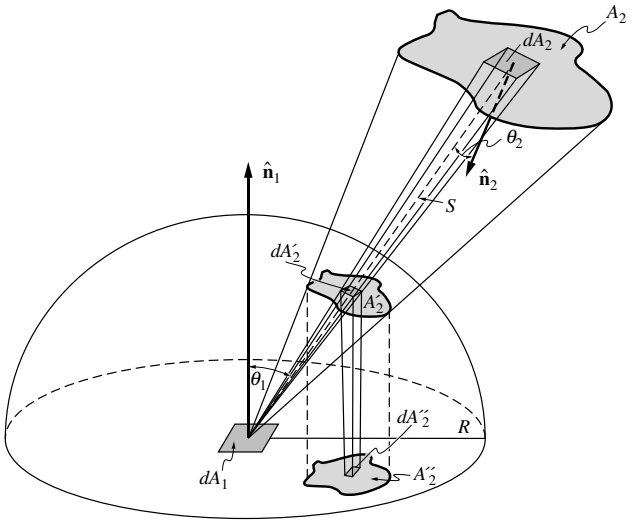

FIGURE 4-21
Surface projection for the unit sphere method.

It remains to find the radius of the sphere R, since only the distance between disks, h, is known. From Fig. 4-20

$$h = \sqrt{R^2 - R_1^2} + \sqrt{R^2 - R_2^2},$$

which may be solved (by squaring twice), to give

$$R^2 = (X^2 - 1)\left(\frac{R_1 R_2}{h}\right)^2, \quad X = \frac{h^2 + R_1^2 + R_2^2}{2R_1 R_2}.$$

This result is, of course, identical to the one given in Example 4.5, although it is not trivial to show this.

4.9 THE UNIT SPHERE METHOD

The unit sphere method is a powerful tool to calculate view factors between one infinitesimal and one finite area. It is particularly useful for the experimental determination of such view factors, as first stated by Nusselt [27]. An experimental implementation of the method through optical projection has been discussed by Farrell [28].

To determine the view factor F_{d1-2} between dA_1 and A_2 we place a hemisphere[2] of radius R on top of A_1, centered over dA_1, as shown in Fig. 4-21. From equations (4.4) and (4.8) we may write

$$F_{d1-2} = \int_{A_2} \frac{\cos\theta_1 \cos\theta_2}{\pi S^2} dA_2 = \int_{\Omega_2} \frac{\cos\theta_1}{\pi} d\Omega_2. \tag{4.53}$$

The solid angle $d\Omega_2$ may also be expressed in terms of area dA_2' (dA_2 projected onto the hemisphere) as $d\Omega_2 = dA_2'/R^2$. Further, the area dA_2' may be projected along the z-axis onto the plane of A_1 as $dA_2'' = \cos\theta_1 \, dA_2'$. Thus,

$$F_{d1-2} = \int_{A_2'} \frac{\cos\theta_1}{\pi} \frac{dA_2'}{R^2} = \int_{A_2''} \frac{dA_2''}{\pi R^2} = \frac{A_2''}{\pi R^2}, \tag{4.54}$$

that is, F_{d1-2} is the fraction of the disk πR^2 that is occupied by the double projection of A_2. Experimentally this can be measured, for example, by placing an opaque area A_2 within a

[2]The name *unit sphere method* originated with Nusselt, who used a sphere of unit radius; however, a sphere of arbitrary radius may be used.

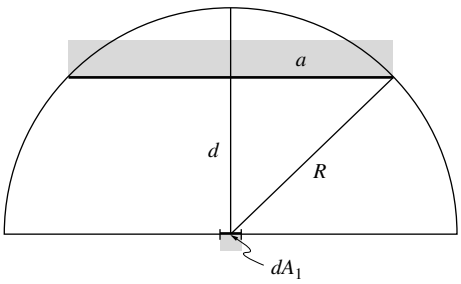

FIGURE 4-22
Geometry for the view factor in Example 4.14.

hemisphere, made of a translucent material, and which has a light source at the center (at dA_1). Looking down onto the translucent hemisphere in the negative z-direction, $A_{2'}$ will appear as a shadow. A photograph of the shadow (and the bright disk) can be taken, showing the double projection of A_2, and F_{d1-2} can be measured.

Example 4.14. Determine the view factor for F_{d1-2} between an infinitesimal area and a parallel disk as shown in Fig. 4-22.

Solution
While a hemisphere of arbitrary radius could be employed, we shall choose here for convenience a radius of $R = \sqrt{a^2 + d^2}$, i.e., a hemisphere that includes the periphery of the disk on its surface. Then $A_2'' = A_2 = \pi a^2$, and the view factor follows as

$$F_{d1-2} = \frac{\pi a^2}{\pi R^2} = \frac{a^2}{a^2 + d^2}.$$

Obviously, only a few configurations will allow such simple calculation of view factors. For a more general case it would be desirable to have some "cookbook formula" for the application of the method. This is readily achieved by looking at the vector representation of the surfaces. Any point on the periphery of A_2 may be expressed as a vector

$$\mathbf{s}_{12} = x\hat{\mathbf{i}} + y\hat{\mathbf{j}} + z\hat{\mathbf{k}}. \tag{4.55}$$

The corresponding point on A_2' may be expressed as

$$\mathbf{s}'_{12} = x'\hat{\mathbf{i}} + y'\hat{\mathbf{j}} + z'\hat{\mathbf{k}} = \frac{R}{\sqrt{x^2 + y^2 + z^2}}\mathbf{s}_{12}, \tag{4.56}$$

and on A_2'' as

$$\mathbf{s}''_{12} = x''\hat{\mathbf{i}} + y''\hat{\mathbf{j}} = x'\hat{\mathbf{i}} + y'\hat{\mathbf{j}}. \tag{4.57}$$

Thus, any point (x, y, z) on A_2 is double-projected onto A_2'' as

$$x_2'' = \frac{x}{\sqrt{x^2 + y^2 + z^2}}R, \quad y_2'' = \frac{y}{\sqrt{x^2 + y^2 + z^2}}R. \tag{4.58}$$

Only the area formed by the projection of the periphery of A_2 through equation (4.58) needs to be found. This integration is generally considerably less involved than the one in equation (4.8).

References

1. Hamilton, D. C., and W. R. Morgan: "Radiant interchange configuration factors," *NACA TN 2836*, 1952.
2. Leuenberger, H., and R. A. Pearson: "Compilation of radiant shape factors for cylindrical assemblies," ASME paper no. 56-A-144, 1956.

3. Kreith, F.: *Radiation Heat Transfer for Spacecraft and Solar Power Design*, International Textbook Company, Scranton, PA, 1962.
4. Sparrow, E. M., and R. D. Cess: *Radiation Heat Transfer*, Hemisphere, New York, 1978.
5. Siegel, R., and J. R. Howell: *Thermal Radiation Heat Transfer*, 4th ed., Taylor and Francis-Hemisphere, Washington, 2002.
6. Howell, J. R.: *A Catalog of Radiation Configuration Factors*, McGraw-Hill, New York, 1982.
7. Howell, J. R., and M. P. Mengüç: "Radiative transfer configuration factor catalog: A listing of relations for common geometries," *Journal of Quantitative Spectroscopy and Radiative Transfer*, vol. 112, pp. 910–912, 2011.
8. Wong, R. L.: "User's manual for CNVUFAC–the General Dynamics heat transfer radiation view factor program," Technical report, University of California, Lawrence Livermore National Laboratory, 1976.
9. Shapiro, A. B.: "FACET–a computer view factor computer code for axisymmetric, 2D planar, and 3D geometries with shadowing," Technical report, University of California, Lawrence Livermore National Laboratory, August 1983, (maintained by Nuclear Energy Agency under http://www.oecd-nea.org/tools/abstract/detail/nesc9578/).
10. Burns, P. J.: "MONTE–a two-dimensional radiative exchange factor code," Technical report, Colorado State University, Fort Collins, 1983.
11. Emery, A. F.: "VIEW–a radiation view factor program with interactive graphics for geometry definition (version 5.5.3)," Technical report, NASA computer software management and information center, Atlanta, 1986, (available from http://www.openchannelfoundation.org/projects/VIEW).
12. Ikushima, T.: "MCVIEW: A radiation view factor computer program or three-dimensional geometries using Monte Carlo method," Technical report, Japan Atomic Energy Research Institute (JAERI), 1986, (maintained by Nuclear Energy Agency under http://www.oecd-nea.org/tools/abstract/detail/nea-1166).
13. Jensen, C. L.: "TRASYS-II user's manual–thermal radiation analysis system," Technical report, Martin Marietta Aerospace Corp., Denver, 1987.
14. Walton, G. N.: "Algorithms for calculating radiation view factors between plane convex polygons with obstructions," in *Fundamentals and Applications of Radiation Heat Transfer*, vol. HTD-72, ASME, pp. 45–52, 1987.
15. Chin, J. H., T. D. Panczak, and L. Fried: "Spacecraft thermal modeling," *Int. J. Numer. Methods Eng.*, vol. 35, pp. 641–653, 1992.
16. Zeeb, C. N., P. J. Burns, K. Branner, and J. S. Dolaghan: "User's manual for Mont3d – Version 2.4," Colorado State University, Fort Collins, CO, 1999.
17. Walton, G. N.: "Calculation of obstructed view factors by adaptive integration," Technical Report NISTIR–6925, National Institute of Standards and Technology (NIST), Gaithersburg, MD, 2002.
18. MacFarlane, J. J.: "VISRAD-a 3D view factor code and design tool for high-energy density physics experiments," *Journal of Quantitative Spectroscopy and Radiative Transfer*, vol. 81, pp. 287–300, 2003.
19. Emery, A. F., O. Johansson, M. Lobo, and A. Abrous: "A comparative study of methods for computing the diffuse radiation viewfactors for complex structures," *ASME Journal of Heat Transfer*, vol. 113, no. 2, pp. 413–422, 1991.
20. Jakob, M.: *Heat Transfer*, vol. 2, John Wiley & Sons, New York, 1957.
21. Liu, H. P., and J. R. Howell: "Measurement of radiation exchange factors," *ASME Journal of Heat Transfer*, vol. 109, no. 2, pp. 470–477, 1956.
22. Wylie, C. R.: *Advanced Engineering Mathematics*, 5th ed., McGraw-Hill, New York, 1982.
23. Moon, P.: *Scientific Basis of Illuminating Engineering*, Dover Publications, New York, 1961, (originally published by McGraw-Hill, New York, 1936).
24. de Bastos, R.: "Computation of radiation configuration factors by contour integration," M.S. thesis, Oklahoma State University, 1961.
25. Sparrow, E. M.: "A new and simpler formulation for radiative angle factors," *ASME Journal of Heat Transfer*, vol. 85, pp. 73–81, 1963.
26. Hottel, H. C.: "Radiant heat transmission," in *Heat Transmission*, ed. W. H. McAdams, 3rd ed., ch. 4, McGraw-Hill, New York, 1954.
27. Nusselt, W.: "Graphische Bestimming des Winkelverhältnisses bei der Wärmestrahlung," *VDI Zeitschrift*, vol. 72, p. 673, 1928.
28. Farrell, R.: "Determination of configuration factors of irregular shape," *ASME Journal of Heat Transfer*, vol. 98, no. 2, pp. 311–313, 1976.

Problems

4.1 For Configuration 11 in Appendix D, find F_{d1-2} by (*a*) area integration, and (*b*) contour integration. Compare the effort involved.

4.2 Using the results of Problem 4.1, find F_{1-2} for Configuration 33 in Appendix D.

4.3 Find F_{1-2} for Configuration 32 in Appendix D, by area integration.

4.4 Evaluate F_{d1-2} for Configuration 13 in Appendix D by (*a*) area integration, and (*b*) contour integration. Compare the effort involved.

4.5 Using the result from Problem 4.4, calculate F_{1-2} for Configuration 40 in Appendix D.

4.6 Find the view factor F_{d1-2} for Configuration 11 in Appendix D, with dA_1 tilted toward A_2 by an angle ϕ.

4.7 Find F_{d1-2} for the surfaces shown in the figure, using (*a*) area integration, (*b*) view factor algebra, and Configuration 11 in Appendix D.

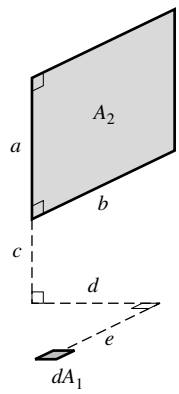

4.8 For the infinite half-cylinder depicted in the figure, find F_{1-2}.

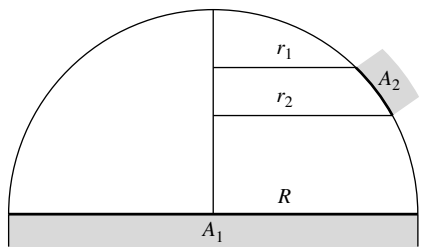

4.9 Find F_{d1-2} for the surfaces shown in the figure.

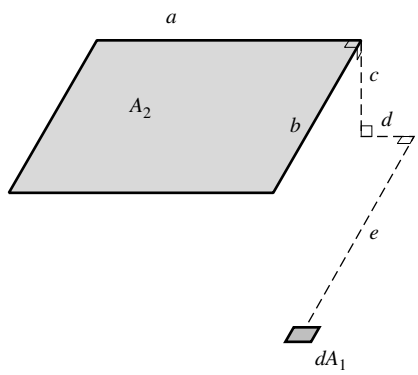

4.10 Find the view factor of the spherical ring shown in the figure to itself, F_{1-1}, using the inside sphere method.

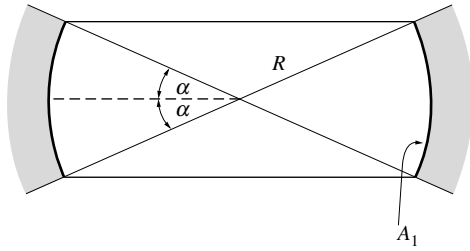

4.11 Determine the view factor for Configuration 51 in Appendix D, using (*a*) other, more basic view factors given in Appendix D, (*b*) the crossed-strings rule.

4.12 To reduce heat transfer between two infinite concentric cylinders a third cylinder is placed between them as shown in the figure. The center cylinder has an opening of half-angle θ. Calculate F_{4-2}.

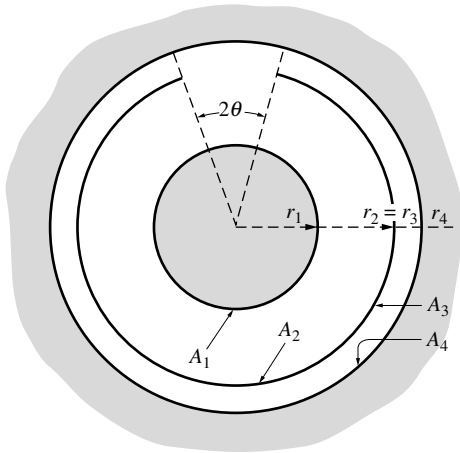

4.13 Consider the two long concentric cylinders as shown in the figure. Between the two cylinders is a long, thin flat plate as also indicated. Determine F_{4-2}.

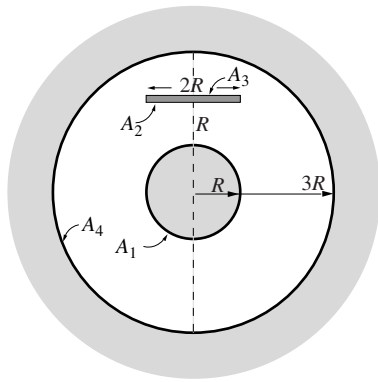

4.14 Calculate the view factor F_{1-2} for surfaces on a cone as shown in the figure.

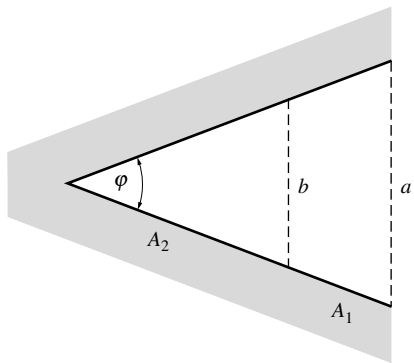

4.15 Determine the view factor F_{1-2} for the configuration shown in the figure, if
(*a*) the bodies are two-dimensional (i.e., infinitely long perpendicular to the paper);
(*b*) the bodies are axisymmetric (cones).

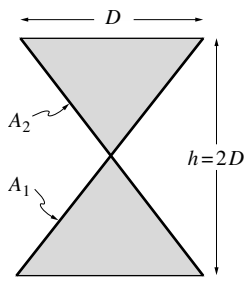

4.16 Consider the configuration shown; determine the view factor F_{1-2} assuming the configuration is

a) axisymmetric (1 is conical, 2 is a disk with a hole), or

b) two-dimensional Cartesian (1 is a V-groove, 2 is comprised of two infinitely long strips).

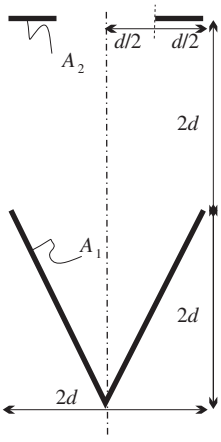

4.17 Find F_{1-2} for the configuration shown in the figure (infinitely long perpendicular to paper).

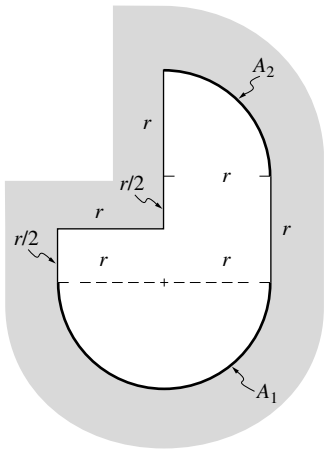

4.18 Calculate the view factor between two infinitely long cylinders as shown in the figure. If a radiation shield is placed between them to obstruct partially the view (dashed line), how does the view factor change?

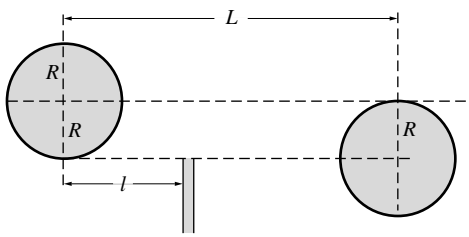

4.19 Find the view factor between spherical caps as shown in the figure, for the case of

$$H \geq \frac{R_1^2}{\sqrt{R_1^2 - a_1^2}} + \frac{R_2^2}{\sqrt{R_2^2 - a_2^2}},$$

where H = distance between sphere centers, R = sphere radius, and a = radius of cap base. Why is this restriction necessary?

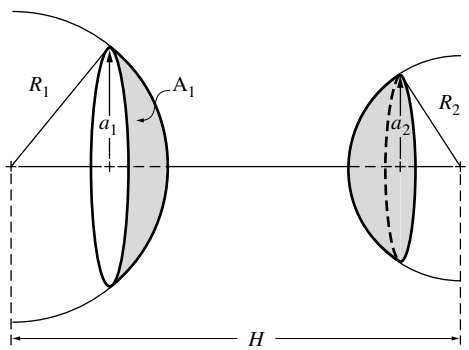

4.20 Determine the view factor for Configuration 18 in Appendix D, using the unit sphere method.

4.21 Consider the axisymmetric configuration shown in the figure. Calculate the view factor F_{1-3}.

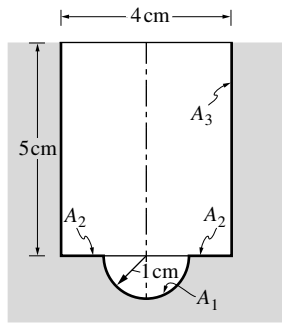

4.22 Find F_{d1-2} from the infinitesimal area to the disk as shown in the figure, with $0 \le \beta \le \pi$.

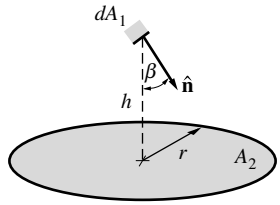

4.23 Consider the configuration shown (this could be a long cylindrical BBQ with a center shelf/hole; or an integrating sphere). Determine the view factors F_{2-2} and F_{2-3} assuming the configuration is

(a) axisymmetric (sphere),

(b) two-dimensional Cartesian (cylinder), using view factor algebra,

(c) two-dimensional Cartesian (cylinder), using the string rule (F_{2-3} only).

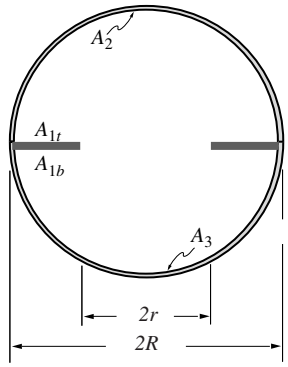

4.24 In the solar energy laboratory at UC Merced parabolic concentrators are employed to enhance the absorption of tubular solar collectors as shown in the sketch. Calculate the view factor from the parabolic concentrator A_1 to collecting cylinder A_2, using

(a) view factor algebra,

(b) Hottel's string rule.

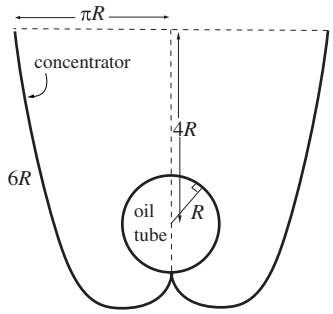

4.25 The interior of a right-circular cylinder of length $L = 4R$, where R is its radius, is to be broken up into 4 ring elements of equal width. Determine the view factors between all the ring elements, using

(a) view factor algebra and the view factors of Configuration 40,

(b) Configuration 9 with the assumption that this formula can be used for rings of finite widths. Assess the accuracy of the approximate view factors. What would be the maximum allowable value for ΔX to ensure that all view factors within a distance of $4R$ are accurate to at least 5%? (Exclude the view factor from a ring to itself, which is best evaluated last, applying the summation rule.) Use the program `viewfactors` or the function `view` in your calculations.

4.26 The inside surfaces of a furnace in the shape of a parallelepiped with dimensions 1 m × 2 m × 4 m are to be broken up into 28 1 m × 1 m subareas. Determine all necessary view factors using the functions `parlplates` and `perpplates` in Appendix F.